Inorganic Chemistry

pubs.acs.org/IC

Article

Structural Diversity and Trends in Properties of an Array of Hydrogen-Rich Ammonium Metal Borohydrides

Jakob B. Grinderslev, Lars H. Jepsen, Young-Su Lee, Kasper T. Møller, Young Whan Cho, Radovan Černý, and Torben R. Jensen*

Cite This: https://dx.doi.org/10.1021/acs.inorgchem.0c01797

Read Online

ACCESS | Metrics & More | Article Recommendations | Supporting Information

ABSTRACT: Metal borohydrides are a fascinating and continuously expanding class of materials, showing promising applications within many different fields of research. This study presents 17 derivatives of the hydrogen-rich ammonium borohydride, NH_4BH_4, which all exhibit high gravimetric hydrogen densities (>9.2 wt % of H_2). A detailed insight into the crystal structures combining X-ray diffraction and density functional theory calculations exposes an intriguing structural variety ranging from three-dimensional (3D) frameworks, 2D-layered, and 1D-chainlike structures to structures built from isolated complex anions, in all cases containing NH_4^+ countercations. Dihydrogen interactions between complex NH_4^+ and BH_4^- ions contribute to the structural diversity and flexibility, while inducing an inherent instability facilitating hydrogen release. The thermal stability of the ammonium metal borohydrides, as a function of a range of structural properties, is analyzed in detail. The Pauling electronegativity of the metal, the structural dimensionality, the dihydrogen bond length, the relative amount of NH_4^+ to BH_4^-, and the nearest coordination sphere of NH_4^+ are among the most important factors. Hydrogen release usually occurs in three steps, involving new intermediate compounds, observed as crystalline, polymeric, and amorphous materials. This research provides new opportunities for the design and tailoring of novel functional materials with interesting properties.

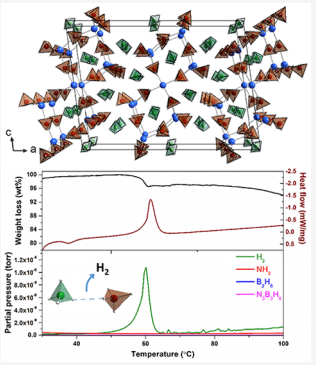

INTRODUCTION

Metal borohydrides have been extensively investigated as potential hydrogen storage materials, and the class of materials has expanded significantly in the past decade. A large number of new mono-, bi-, and trimetallic borohydrides have been reported, which have unveiled a fascinatingly large structural flexibility and a wide range of compositions.[1−3] The class of materials has been further expanded by anion substitution with e.g. NH_2^- or halides or by addition of neutral ligands such as NH_3, $NH_3{\cdot}BH_3$, and $S(CH_3)_2$.[2,4−19] In addition to the high hydrogen densities, a number of other applications and properties have been investigated in recent years. Interesting magnetic properties were discovered for the rare-earth-metal borohydrides,[4,20,21] which may show applications for magnetic refrigeration,[21] and magnetic superexchange through a borohydride group was discovered for the first time in α-$Gd(BH_4)_3$.[4] A high ionic conductivity is observed in the high-temperature polymorph of $LiBH_4$ above $T \approx 115$ °C, which initiated the investigation of complex metal hydrides as solid-state ionic conductors. Recently it has been demonstrated that addition of a neutral molecule to a metal borohydride could be a new approach to achieve superionic conductivity at low temperatures, as observed for $LiBH_4{\cdot}xNH_3$ (x = 1/2, 1),[22,23] $LiBH_4{\cdot}xNH_3BH_3$ (x = 1/2, 1),[24] $Mg(BH_4)_2{\cdot}xNH_3$ (x = 1−6),[25] $Mg(BH_4)_2{\cdot}xNH_2CH_2CH_2NH_2$ (x = 1, 3),[26] $Mg(BH_4)_2{\cdot}x$(diglyme) (x = 1/2, 1),[27] and $Mg(BH_4)_2{\cdot}2NH_3BH_3$.[28,29] Favorable luminescent properties are discovered in the metal borohydride solvates $M(BH_4)_2{\cdot}2THF$ (M = Eu, Yb) and in several perovskite-type metal borohydrides, due to the large spatial separation by the BH_4^- groups, which suppresses quenching effects.[30,31] Other potential applications of metal borohydrides involve gas adsorption, as demonstrated for the porous γ-$Mg(BH_4)_2$,[32,33] as explosives via a reaction with sulfur,[34] as precursors for metal borides,[35] and as reducing agents in organic chemistry,[36,37] while the main focus has been on ionic conductors and for hydrogen storage.[38−40] Thus, metal borohydrides are indeed a fascinating class of materials, which have prompted the present investigation of new bicationic borohydrides.

Bimetallic borohydrides are frequently formed in the reaction between alkali-metal borohydrides and other metal borohydrides, in particular for the heavier alkali metals (M = K, Rb, Cs).[2] The majority of the bimetallic borohydrides are formed by ball milling of either the two metal borohydrides[21,41−50] or the alkali-metal borohydride and a metal chloride.[51−61] Alternatively, bimetallic borohydrides may also be obtained via solvent-mediated synthesis.[62,63] The majority

Received: June 17, 2020

https://dx.doi.org/10.1021/acs.inorgchem.0c01797
Inorg. Chem. XXXX, XXX, XXX−XXX

Table 1. Overview of Selected Syntheses and the Compositions of the Samples Extracted by Analysis of Diffraction Data

sample	reactants	ratio	crystalline product(s) as synthesized(mol %)[b]
Li12	NH_4BH_4 + $LiBH_4$	1:2	$NH_4Li(BH_4)_2$ (49.2%), $NH_4Li_2(BH_4)_3$ (2.3%), $LiBH_4$ (48.5%),
Li11[a]	NH_4BH_4 + $LiBH_4$	1:1	$NH_4Li(BH_4)_2$ (91.3%), NH_4BH_4 (8.7%)
Na11	NH_4BH_4 + $NaBH_4$	1:1	NH_4BH_4 (6.1%), $NaBH_4$ (77.1%), $((NH_3)_2BH_2)BH_4$ (16.8%)
Mg11	NH_4BH_4 + $Mg(BH_4)_2$	1:1	$(NH_4)_2Mg(BH_4)_4$, α-$Mg(BH_4)_2$, Mg1
Mg21	NH_4BH_4 + $Mg(BH_4)_2$	2:1	$(NH_4)_3Mg(BH_4)_5$, Mg1[c]
Mg31	NH_4BH_4 + $Mg(BH_4)_2$	3:1	$(NH_4)_3Mg(BH_4)_5$ (40.3%), $NH_4Mg(BH_4)_3{\cdot}2NH_3$ (24.8%), NH_3BH_3 (26.7%), NH_4BH_4 (8.2%)
Ca11	NH_4BH_4 + $Ca(BH_4)_2$	1:1	$NH_4Ca(BH_4)_3$
Sr11a	NH_4BH_4 + $Sr(BH_4)_2$	1:1	$NH_4Sr(BH_4)_3$ (83.3%). SrH_2 (16.7%)
Sr11b	NH_4BH_4 + $Sr(BH_4)_2$	1:1	$NH_4Sr(BH_4)_3$. Sr2[c]
Mn11[a]	NH_4BH_4 + $Mn(BH_4)_2$	1:1	$(NH_4)_2Mn(BH_4)_4$ (21.4%), $Mn(BH_4)_2$ (21.7%), NH_4BH_4 (42.1%), LiCl (14.8%), Mn1[c]
Mn21[a]	NH_4BH_4 + $Mn(BH_4)_2$	2:1	$(NH_4)_3Mn(BH_4)_5$ (37.9%), $LiMn(BH_4)_3{\cdot}2NH_3$ (6.8%), NH_4BH_4 (42.8%), LiCl (12.5%), Mn2[c]
Mn31[a]	NH_4BH_4 + $Mn(BH_4)_2$	3:1	$(NH_4)_3Mn(BH_4)_5$ (21.4%), $NH_4Mn(BH_4)_3{\cdot}2NH_3$ (5.2%), NH_4BH_4 (66.6%), LiCl (6.9%)
Y11	NH_4BH_4 + $Y(BH_4)_3$	1:1	$NH_4Y(BH_4)_4$ (80.7%), α-$Y(BH_4)_3$ (17.1%), β-$Y(BH_4)_3$ (2.2%)
Y21	NH_4BH_4 + $Y(BH_4)_3$	2:1	$NH_4Y(BH_4)_4{\cdot}NH_3$ (81.2%), $(NH_4)_2Y(BH_4)_5{\cdot}NH_3$ (18.8%), Y1[c]
La11	NH_4BH_4 + $La(BH_4)_3$	1:1	$(NH_4)_3La_2(BH_4)_9$ (50.8%), $La(BH_4)_3$ (49.2%)
La31	NH_4BH_4 + $La(BH_4)_3$	3:1	$(NH_4)_3La(BH_4)_6$ (84.8%), $NH_4La(BH_4)_4{\cdot}NH_3$ (11.4%), $(NH_4)_2La(BH_4)_5{\cdot}NH_3BH_3$ (3.8%),
Gd11	NH_4BH_4 + $Gd(BH_4)_3$	1:1	$(NH_4)_2Gd(BH_4)_5$ (17.0%), $Gd(BH_4)_3$ (83.0%)
Gd21	NH_4BH_4 + $Gd(BH_4)_3$	2:1	$NH_4Gd(BH_4)_4{\cdot}NH_3$ (59.2%), $(NH_4)_2Gd(BH_4)_5$ (40.8%)
Gd31	NH_4BH_4 + $Gd(BH_4)_3$	3:1	$NH_4Gd(BH_4)_4{\cdot}NH_3$ (62.5%), $(NH_4)_2Gd(BH_4)_5$ (13.5%), $(NH_4)_3Gd(BH_4)_6$ (24.1%)

[a]Prepared in small cryo sample vials (2 mL). [b]Mole percent determined from Rietveld refinements. [c]Minor phase.

of the bimetallic borohydrides consist of complex anions formed by the more electronegative metal cation and the borohydride groups, which is charge-balanced by the less electronegative alkali-metal ion. The bonds between the alkali-metal counterion and the BH_4^- are ionic in character, while the bonds between the more electronegative metal and the BH_4^- are more covalent.[1,2] The complex anions often exist as isolated anions[47,48,50,53,56,58−61,64,65] or as 3D frameworks via bridging BH_4^- groups.[21,31,41,42,48,52] One-dimensional (1D) chainlike structures and 2D-layered structures among the bimetallic borohydrides are only observed as Li−BH_4 frameworks in the $LiBH_4$−MBH_4 systems (M = K, Rb, Cs).[1,49]

The decomposition temperature of the first bimetallic borohydride, $LiK(BH_4)_2$, was found to be between those of the pristine compounds, possibly due to the formation of a eutectic melt.[66,67] However, for the remaining bimetallic borohydrides the stability was governed by the more electronegative metal forming the complex anion. Thus, the bimetallic borohydrides dissociate into the monometallic borohydrides when the temperature approaches that of the decomposition temperature of the less stable metal borohydride, and the two monometallic borohydrides decompose as the pristine compounds.[41,42,48,51,61]

Ammonium borohydride, NH_4BH_4, has the highest gravimetric (24.5 wt % H_2) and volumetric hydrogen density (157.0 g H_2/L) among the known inorganic compounds. The latter value is more than twice the density of liquid hydrogen (71 g/L). NH_4BH_4 releases 75% of its H_2 content in three distinct exothermic reactions below 160 °C.[68] However, NH_4BH_4 is metastable at room temperature with a half-life of ∼6 h and decomposes into the diammoniate of diborane, $[(NH_3)_2BH_2]BH_4$,[68−70] via a release of hydrogen, and also toxic gases such as ammonia and borazine. NH_4BH_4 crystallizes in a rock-salt structure type at room temperature, which consists of the hydrogen disordered complex ions NH_4^+ and BH_4^-. The presence of hydridic $H^{\delta-}$ and protonic $H^{\delta+}$ gives rise to intermolecular dihydrogen bonding, which has been subjected to recent investigations by inelastic and quasi-elastic neutron scattering.[71]

The first bicationic borohydride was based on NH_4BH_4 and $Ca(BH_4)_2$, resulting in the perovskite-type compound $NH_4Ca(BH_4)_3$, isostructural with the Rb and Cs analogues.[31] $NH_4Ca(BH_4)_3$ effectively stabilizes NH_4BH_4 and decomposes into $Ca(BH_4)_2{\cdot}NH_3BH_3$ via an exothermic hydrogen release at $T \approx 100$ °C.[16,31] Later the structures and thermal properties of $NH_4M(BH_4)_4$ (M = Al, Sc, Y) and $(NH_4)_3Mg(BH_4)_5$ were reported, which appear to decompose at lower temperatures in comparison to NH_4BH_4.[72−74] $NH_4M(BH_4)_4$ (M = Sc, Y) are isostructural with $RbY(BH_4)_4$ and $(NH_4)_3Mg(BH_4)_5$ is isostructural with the Rb and Cs analogues, while $NH_4Al(BH_4)_4$ is isostructural with the K analogue.[72−74] The compounds decompose in exothermic reactions, releasing mainly H_2, but also other gases such as B_2H_6 and in some cases NH_3 and $N_3B_3H_6$.[72−74] However, the samples (except for M = Al) were prepared from halide precursors and contain significant amounts of LiCl and other byproducts, which may hamper an analysis of the crystal structure and other properties.

Here we further expand the family of ammonium metal borohydrides and provide new insight into the crystal structures and thermal properties of ammonium metal borohydrides. The compounds investigated here were prepared using high-purity metal borohydride precursors, which allowed for a more detailed characterization. Here we present 17 new high-hydrogen-capacity materials, and the crystal structures have been analyzed in detail by combined *in situ* variable-temperature synchrotron powder X-ray diffraction (SR PXD) and density functional theory (DFT) calculations along with thermal analysis and Fourier transform infrared spectroscopy (FT-IR). Furthermore, the thermal stability is analyzed relative to a range of structural properties.

EXPERIMENTAL SECTION

Sample Preparation. Ammonium borohydride, NH_4BH_4, was prepared by following previously published procedures.[75] NH_4F (10% molar excess, ≥99.99%, Sigma-Aldrich) and $NaBH_4$ (Sigma-Aldrich) were reacted in liquid NH_3 at $T = -78$ °C (dry ice and ethanol). NH_4BH_4 is formed after 4 h at $T = -78$ °C with continuous stirring,

https://dx.doi.org/10.1021/acs.inorgchem.0c01797
Inorg. Chem. XXXX, XXX, XXX−XXX

and the byproducts, NaF and unreacted NH_4F, were removed by filtration. Excess and coordinated NH_3 was removed under vacuum at $T = -40$ °C to recover NH_4BH_4. The metal borohydrides $LiBH_4$ and $NaBH_4$ were purchased from Sigma-Aldrich, while the solvent- and chloride-free metal borohydrides $Mg(BH_4)_2$, $Ca(BH_4)_2$, $Sr(BH_4)_2$, $Mn(BH_4)_2$, $Y(BH_4)_3$, $La(BH_4)_3$, and $Gd(BH_4)_3$ were synthesized in-house by combining solvent-based methods and mechanochemistry according to previously described protocols.[5,75−77]

Cryo mechanochemistry ($T = -196$ °C) of NH_4BH_4−$M(BH_4)_m$ (M = Li, Na, Mg, Ca, Sr, Y, La, Gd) in appropriate ratios (see Table 1) was carried out using a 6770 Spex Freezer mill. The powders were loaded in a polycarbonate cylinder (25 mL) or a stainless steel cylinder (2 mL), in both cases with stainless steel end plugs and a stainless steel rod. The canister was magnetically rotated back and forth 15 times per second for 2 min intervened by a 2 min break, and this sequence was repeated 15 times.

A Note on Safety. All reagents and starting materials are air- and moisture-sensitive and may react violently with H_2O. All sample handling and preparation was performed under an inert argon atmosphere using Schlenk techniques or using an argon-filled glovebox with a circulation purifier, $p(O_2, H_2O) < 1$ ppm. The materials are thermally sensitive and should be stored in a glovebox freezer (below $T = -34$ °C), and samples should be kept cold during handling.

Synchrotron Radiation Powder X-ray Diffraction. *In situ* variable-temperature synchrotron radiation powder X-ray diffraction data (SR PXD) were collected at the BM01 beamline at the European Synchrotron Radiation Facility (ESRF, Grenoble, France) with wavelengths $\lambda = 0.69449$ and $\lambda = 0.8212$ Å, at the beamline I11 at the Diamond Light Source (Oxford, England) with wavelengths $\lambda = 0.825775$ and $\lambda = 0.825873$ Å, and at the beamline I711 at MAXII, MAX-Lab (Lund, Sweden) with the wavelength $\lambda = 0.9938$ Å. The samples were packed in 0.5 mm boron silicate capillaries, sealed under an argon atmosphere, and heated at a heating rate of 2−5 °C/min in the temperature range $T = -25$ to +500 °C. The samples were rotated during data acquisition.

Structural Solution and Refinement. The crystal structures were solved and refined from SR PXD data. The general procedure involved indexing of the unit cell and subsequently solving the structure *ab initio* by global optimization in direct space, as implemented in the program FOX, and treating BH_4^-, NH_4^+, NH_3, and NH_3BH_3 as rigid bodies during the structure solution process.[78] The structural model was then refined by the Rietveld method using the program Fullprof[79] and was checked for higher symmetry using the ADDSYM routine in Platon.[80]

Verification of the structural models was performed by evaluating the structure after Rietveld refinements, where a poor fit to the PXD data and unreasonable bond distances indicated a wrong structural model. In these cases, a new structural model and in some cases modified composition was attempted to obtain a better fit to the observed PXD data.

In the metal coordination sphere it is particularly challenging to distinguish the ligands NH_3 and BH_4^-, as they are isoelectronic and often have similar bond distances to the metal. Thus, permutations of the ligands coordinating the metal were considered, and the most likely configuration was selected, considering both chemical properties and the results from DFT optimization. The coordinations of NH_3 and BH_4^- are different, since NH_3 always coordinates to the metal via the nitrogen lone pair as a terminal ligand, while BH_4^- may act as a bridging ligand between two metal atoms. Furthermore, N−H usually forms dihydrogen bonds to nearby BH_4^- complexes. All of the structures containing NH_3 also contain terminal BH_4^- ligands; thus permutations other than those presented here may be possible.

DFT calculations were used for a final verification of the structural models, and large deviations in the unit cell volume and atomic positions indicated a wrong structural model. Crystallographic information files (CIF) are reported for the DFT-optimized structures. The atomic positions were not refined in subsequent Rietveld refinements after DFT optimization.

Density Functional Theory Calculations. The experimental structures were optimized by DFT calculations. The calculations were performed using the Vienna Ab initio Simulation Package (VASP)[81] with van der Waals density functional (vdW-DF2) proposed by Lee et al.[82,83] The inclusion of van der Waals energy gives a better prediction of the lattice parameters for systems with weak bonds as in this work. A projector-augmented wave potential[84] with a plane-wave cutoff energy of 500 eV was used, and the unit cell parameters were optimized using a higher plane-wave cutoff energy of 600 eV. As a measure of agreement between the experimental structure solution and the calculated structure, cell parameters and cell volumes are compared in Table S1 and Figure S1.

Fourier Transform Infrared Spectroscopy (FTIR). The samples were characterized by infrared absorption spectroscopy using a NICOLET 380 FT-IR spectrometer from Thermo Electron Corporation with a diamond attenuated total reflectance (ATR) crystal. The samples were exposed to air for approximately 10 s when they were transferred from the sample vial to the instrument. Data were collected in the range 500−4000 cm^{-1}, and 32 scans with a spectral resolution of 4 cm^{-1} were collected per sample and averaged.

Thermal Analysis and Mass Spectroscopy. Thermogravimetric analysis (TGA) and differential scanning calorimetry (DSC) were measured using a PerkinElmer STA 6000 coupled with a mass spectrometer (MS) (Hiden Analytical HPR-20 QMS sampling system). Each sample (approximately 1−5 mg) was placed in an Al_2O_3 crucible and heated with a rate of 2−5 °C/min and an argon purge rate of 20 mL/min. The outlet gas was monitored for hydrogen ($m/z = 2$), ammonia ($m/z = 17$), diborane ($m/z = 26$), and borazine ($m/z = 80$) using mass spectrometry.

Temperature-Programmed Photographic Analysis (TPPA). Samples were sealed under argon in a glass tube placed in a custom-made oven as described in the literature.[85] The samples were heated from room temperature to 400 °C with a heating rate of 5 °C/min, while photos of the sample were collected every 5 s.

RESULTS AND DISCUSSION

Synthesis and Initial Characterization. Extensive systematic synthesis work has allowed the preparation of 10 novel ammonium metal borohydrides and 7 ammonium metal borohydride derivatives by combining ammonium borohydride, NH_4BH_4, and metal borohydrides, $M(BH_4)_m$ (M^{m+} = Li^+, Na^+, Mg^{2+}, Ca^{2+}, Sr^{2+}, Mn^{2+}, Y^{3+}, La^{3+}, Gd^{3+}, according to the addition reaction in eq 1, using a cryo-mechanochemical approach.[86]

$$x\mathrm{NH_4BH_4(s)} + y\mathrm{M(BH_4)_m(s)} \xrightarrow{-196\ ^\circ\mathrm{C}} (\mathrm{NH_4})_x\mathrm{M_y(BH_4)_{x+my}(s)} \quad (1)$$

The precursors, ammonium borohydride and metal borohydrides, were prepared as solvent- and halide-free compounds.[5,75−77] The synthesis conditions provide products according to eq 1, but small amounts of remaining reactants and/or decomposition products are often present. Further optimization of the synthesis conditions may improve the purity of the samples. In some cases the reaction partially occurs during the cryo-mechanochemical treatment and partially during the thermal treatment (i.e., observed during an *in situ* SR PXD investigation). NH_4BH_4 gradually decomposes during extended cryo-mechanical treatment to $[(NH_3)_2BH_2][BH_4]$. However, if a stable ammonium metal borohydride is not formed with a composition that matches the initial ratio between $M(BH_4)_m$ and NH_4BH_4 (with NH_4BH_4 in excess), then an ammonium metal borohydride derivative may be formed, containing neutral molecules such as NH_3 and/or NH_3BH_3 due to partial decomposition: e.g., $NH_4Y(BH_4)_4{\cdot}NH_3$ and $(NH_4)_2Y(BH_4)_5{\cdot}NH_3$ are formed in

https://dx.doi.org/10.1021/acs.inorgchem.0c01797
Inorg. Chem. XXXX, XXX, XXX−XXX

Table 2. Overview of Compounds Investigated in This Study[a]

compound	crystal system	space group	a (Å)	b (Å)	c (Å)	β (deg)	V (Å^3)	T (°C)	ref
NH_4BH_4	cubic	$Fm\bar{3}m$	6.95530(4)				336.471(4)	−23	68
$NH_4Li(BH_4)_2$	monoclinic	$C2/m$	23.6459(6)	4.57158(9)	17.2327(4)	97.740(1)	1845.86(7)	53	*b*
$NH_4Li_2(BH_4)_3$	hexagonal	$P6_222$	7.5220(1)		11.6918(2)		572.91(2)	54	*b*
$(NH_4)_2Mg(BH_4)_4$	monoclinic	$P2_1/c$	8.3101(3)	10.0611(3)	14.1360(6)	115.591(2)	1065.95(7)	−23	*b*
$(NH_4)_3Mg(BH_4)_5$	tetragonal	$I4/mcm$	9.1462(3)		16.1920(6)		1354.52(8)	−20	74
$NH_4Ca(BH_4)_3$	cubic	$Pm\bar{3}m$	5.630(1)				178.49(7)	−23	31
$NH_4Sr(BH_4)_3$	cubic	$Pm\bar{3}m$	5.782(1)				193.26(7)	−183	*b*
$NH_4Y(BH_4)_4$	monoclinic	$P2_1/c$	8.1094(2)	12.2544(3)	13.1896(3)	127.5866(8)	1038.65(4)	33	72
$(NH_4)_2Mn(BH_4)_4$	monoclinic	$P2_1/c$	8.3075(2)	10.0701(2)	14.4389(4)	115.942(1)	1086.21(4)	62	*b*
$(NH_4)_3Mn(BH_4)_5$	tetragonal	$I4/mcm$	9.2635(2)		16.1898(3)		1389.28(4)	50	*b*
$(NH_4)_3La_2(BH_4)_9$	trigonal	$R3$	8.0207(1)		30.4550(6)		1696.73(5)	71	*b*
$(NH_4)_3La(BH_4)_6$	monoclinic	$P2_1$	8.1271(2)	8.4688(2)	11.8023(2)	90.272(1)	812.30(3)	51	*b*
$(NH_4)_2Gd(BH_4)_5$	monoclinic	$P2_1/m$	8.8175(2)	12.4141(3)	12.1332(3)	105.18(0)	1281.8(5)	23	*b*
$(NH_4)_3Gd(BH_4)_6$	monoclinic	$P2_1$	8.0611(8)	8.3933(8)	11.718(1)	90.38(1)	792.8(1)	44	*b*
$NH_4Mg(BH_4)_3{\cdot}2NH_3$	hexagonal	$P6_3/m$	8.4754(3)		8.2517(3)		513.33(3)	37	*b*
$NH_4Mn(BH_4)_3{\cdot}2NH_3$	hexagonal	$P6_3/m$	8.4808(2)		8.2573(3)		514.33(3)	−3	*b*
$NH_4Y(BH_4)_4{\cdot}NH_3$	orthorhombic	$Pca2_1$	13.0165(5)	8.0587(3)	10.5784(4)		1109.63(7)	27	*b*
$(NH_4)_2Y(BH_4)_5{\cdot}NH_3$	cubic	$Fm\bar{3}$	11.2882(7)				1438.4(2)	27	*b*
$NH_4La(BH_4)_4{\cdot}NH_3$	hexagonal	$P6_3cm$	15.0019(4)		8.5961(3)		1675.43(8)	55	*b*
$(NH_4)_2La(BH_4)_5{\cdot}NH_3BH_3$	monoclinic	$P2_1$	8.2966(8)	11.1498(8)	8.2958(7)	95.54(0)	763.8(3)	44	*b*
$NH_4Gd(BH_4)_4{\cdot}NH_3$	hexagonal	$P6_3cm$	14.7839(4)		8.2325(3)		1558.26(8)	50	*b*

[a]All unit cell parameters are extracted from Rietveld refinement of SR PXD data. [b]New compositions and structures discovered in this work.

the reaction between NH_4BH_4 and $Y(BH_4)_3$ in a molar ratio of 2:1.

An overview of the conducted syntheses is provided in Table 1, while all of the new compounds discovered in this investigation are provided in Table 2. A concise description and Rietveld refinements of all crystal structures are provided in Figures S2−S31 in the Supporting Information. Thermal decomposition of these new compounds produces a variety of other new crystalline or partially amorphous compounds, four of which have been indexed (Table S2). FT-IR reveals similar features for the ammonium metal borohydrides (Figure S32). The characteristic bands can be assigned to N−H stretching (~2900−3500 cm^{-1}), N−H bending (~1200−1700 cm^{-1}), B−H stretching (~1900−2550 cm^{-1}), and B−H bending (~900−1450 cm^{-1}) modes.[87,88]

Structural Analysis. Indexing and structural analysis reveals a systematic correlation between composition and unit cell volume: $V/Z((NH_4)_xM_y(BH_4)_{x+my}) \approx xV/Z(NH_4BH_4) + yV/Z(M(BH_4)_m)$. Interestingly, the new compounds are often more compact than the volume of the reactants, as suggested by this simple relation (Figure 1). This is likely due to a more efficient packing in the crystal structure and the extended dihydrogen-bonding network that is formed.

The ammonium metal borohydrides exhibit extreme hydrogen densities, exceeding those of many well-known hydrogen-rich compounds, and a significantly higher volumetric hydrogen density in comparison to liquid H_2 (see Figure 2). Notice that many of the compounds have volumetric hydrogen densities exceeding twice that of pure liquid hydrogen (ρ_v > 142 g H_2/L) and are also about 50% higher than that of liquid natural gas and liquid ammonia. The structures of the ammonium metal borohydrides are diverse and fascinating. The tetrahedral geometry of the isoelectronic cations and anions, BH_4^- and NH_4^+, and the dihydrogen bonds between partially positive $H^{\delta+}$ in NH_4^+ and partially negative $H^{\delta-}$ in BH_4^-, i.e. $N-H^{\delta+}\cdots{}^{-\delta}H-B$, lead to unexpected crystal structures and properties.[71] Although they are weak, typically

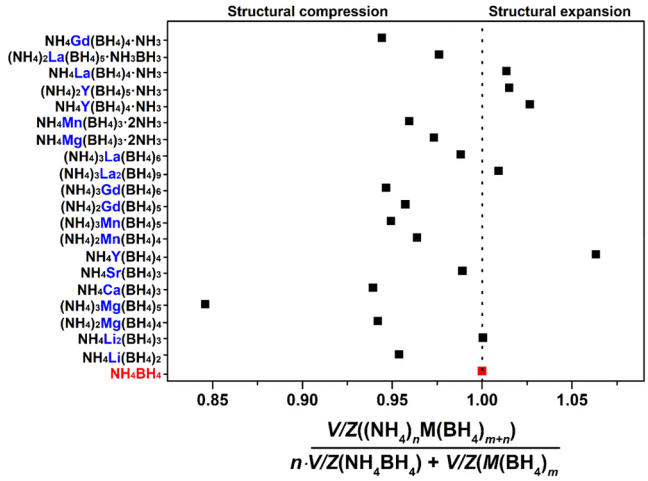

Figure 1. Relative expansion or compression of the ammonium metal borohydrides and derivatives in comparison to the volume per formula unit (V/Z) of the reactants (the V/Z values are obtained from experimental diffraction data).

in the range 13−29 kJ/mol, and often have a length of about 2 Å,[25,89] dihydrogen bonds are important in determining the structure and properties of the compounds: e.g., NH_3BH_3 is a solid under ambient conditions due to the presence of dihydrogen bonds (in contrast to the monomers, NH_3 and B_2H_6, which are gases).[89] The metal borohydrides are often structurally related to metal oxides due to the isoelectronic anions BH_4^- and O^{2-}.[1,2] Repulsive homopolar hydrogen interactions in the metal borohydrides (between BH_4^- complexes) influence the crystal structures in order to maximize the H−H distance.[31,90] In contrast, the introduction of NH_4^+ may influence the crystal structure symmetry due to the formation of favorable dihydrogen bonds to BH_4^- and thereby acts as a potential tool to tailor the properties of new

https://dx.doi.org/10.1021/acs.inorgchem.0c01797
Inorg. Chem. XXXX, XXX, XXX−XXX

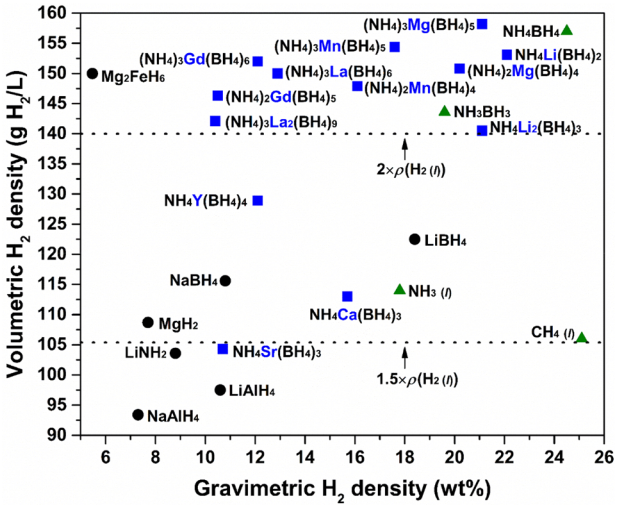

Figure 2. Volumetric and gravimetric hydrogen densities of ammonium metal borohydrides in comparison to selected hydrogen-rich compounds and liquid hydrogen ($\rho(H_2)$ = 71 g H_2/L, black dotted lines). Color code: ammonium metal borohydrides investigated in this study (blue squares), selected complex metal hydrides (black circles), and other hydrogen-rich compounds, NH_3(l), CH_4(l), NH_3BH_3(s), and NH_4BH_4(s) (green triangles).

functional materials, which cannot be obtained using the less directional halides or alkali-metal ions.

The coordination geometry and structural analogues are presented in Table 3. The structures of monometallic borohydrides, $M(BH_4)_m$ (M^{m+} = Li^+, Mg^{2+}, Ca^{2+}, Sr^{2+}, Mn^{2+}, Y^{3+}, La^{3+}, Gd^{3+}), consist of 3D networks of $[M(BH_4)_4]$ tetrahedra or $[M(BH_4)_6]$ octahedra, where BH_4^- acts as a bridging ligand, in most cases coordinating through the edge of the BH_4^- tetrahedron (κ^2).[1,2] Introduction of NH_4BH_4 into $M(BH_4)_m$ interrupts these frameworks, forming new structures with isolated complex ions (0D), 1D chains, 2D layers, or 3D frameworks (see Figure 3). Structures with lower dimensionality (0D, 1D, and 2D) are interconnected by the dihydrogen-bond network, resulting in much shorter dihydrogen bonds, ~1.59−1.82 Å, in comparison to the 3D-framework structures, ~2.18−2.29 Å, which are interconnected by the bridging BH_4^- groups. The crystal structures of the ammonium metal borohydrides can in some cases be related to the structures of bimetallic potassium- or rubidium-based borohydrides, due to the similar ionic radii: $r(NH_4^+)$ = 1.48 Å, $r(K^+)$ = 1.38 Å, and $r(Rb^+)$ = 1.52 Å.[91,92] However, in contrast to the spherical alkali-metal ions, the NH_4^+ ion has more directionality. In the crystal structures described here, NH_4^+ is considered as a counterion in the solid state, while the BH_4^- complex has a more flexible coordination as a ligand and may also act as a counterion, as discussed in the following.

Three-Dimensional Structures. 3D networks of bridging M−BH_4−M are observed in the perovskite-type structures, $NH_4M(BH_4)_3$ (M^{2+} = Ca, Sr), which are built from shared $[M(BH_4)_6)]$ octahedra (Figure 4a). Due to the smaller size of Li^+, the 3D network in $NH_4Li_2(BH_4)_3$ consists of shared $[Li(BH_4)_4]$ tetrahedra, where BH_4^- complexes connect two or four Li^+, which is significantly different in comparison to $LiBH_4$. As already discussed in ref 49, this is the only nonperovskite 3D framework among double-cation borohydrides containing the Li−BH_4 framework. The stability of the framework is high, as it also exists for the Rb and Cs analogues.[49]

Two-Dimensional Structures. A new structure type is observed for $(NH_4)_3La_2(BH_4)_9$, which is also the first observation of a compound with the composition $(M^+)_3(M^{3+})_2(BH_4)_9$. The structure is built from shared $[La(BH_4)_6]$ octahedra, which form 2D layers (Figure 4b). The NH_4^+ groups have irregular 12-fold coordination (to BH_4^-) derived from a cuboctahedron, with one group taking part of the 2D layer and two other groups connecting the layers.

One-Dimensional Structures. The structure of $NH_4Li(BH_4)_2$ consists of (4,4)-connected chains, interconnected along the *b* axis, forming an infinite chain running along the *b* axis (Figure 4c). In this structure, Li^+ is coordinated in both tetrahedral and square planar modes by four edge-sharing BH_4^- (κ^2). The NH_4^+ groups have 8-fold coordination, with one group situated in the (4,4)-connected chain and three groups connecting the chains.

Zero-Dimensional Structures with Isolated Complexes. The majority of the ammonium metal borohydrides form structures with isolated complex ions, as observed for $(NH_4)_2M(BH_4)_4$ (M^{2+} = Mg, Mn) and $NH_4Y(BH_4)_4$, which consist of $[M(BH_4)_4]$ tetrahedra. Similarly, the structures of $(NH_4)_3M(BH_4)_5$ (M^{2+} = Mg, Mn) consist of $[M(BH_4)_4]$ tetrahedra, while one BH_4^- group acts as a negative counterion. The compounds $(NH_4)_3M(BH_4)_6$ (M^{3+} = La, Gd) form double-perovskite-type structures where the metal is octahedrally coordinated to six BH_4^- groups. Several compounds are known with the composition $M^+M^{3+}(BH_4)_4$ (M^+ = Li, Na, K; M^{3+} = Y, Sc, Yb, Lu, Gd).[2] On the other hand, $K_2Gd(BH_4)_5$ is the only reported compound with the composition $(M^+)_2M^{3+}(BH_4)_5$, which is stable because Gd^{3+} has the ability to obtain 5-fold coordination with BH_4^-, in contrast to other rare-earth-metal borohydrides reported so far.[2,4,21] The crystal structure of $(NH_4)_2Gd(BH_4)_5$ consists of isolated complex units of $[Gd(BH_4)_5]$ with both trigonal-bipyramidal and square-pyramidal coordination geometries of Gd^{3+}. Selected crystal structures and coordination geometries of structures with isolated complexes are illustrated in Figure 5.

Derivatives of Ammonium Metal Borohydrides. The structures of $NH_4M(BH_4)_3{\cdot}2NH_3$ (M = Mg, Mn) and $NH_4Y(BH_4)_4{\cdot}NH_3$ consist of ionic complexes of $[M(NH_3)_2(BH_4)_3]^-$ (M = Mg, Mn) or $[Y(NH_3)(BH_4)_4]^-$, where the metal is coordinated in a trigonal-bipyramidal fashion by five ligands, while the structures of $(NH_4)_2Y(BH_4)_5{\cdot}NH_3$ and $(NH_4)_2La(BH_4)_5{\cdot}NH_3BH_3$ consist of ionic complexes of $[Y(NH_3)(BH_4)_5]^{2-}$ or $[La(NH_3BH_3)(BH_4)_5]^{2-}$, where the metal is octahedrally coordinated by six ligands. In contrast, the structures of $NH_4M(BH_4)_4{\cdot}NH_3$ (M = La, Gd) form 1D zigzag chains of connected $[M(NH_3)(BH_4)_5]$ octahedra along the *c* axis.

Flexibility of the Borohydride Ligand. In crystal structures containing NH_3, the NH_3 ligand always coordinates to the metal via the nitrogen lone pair, in contrast to the weakly coordinating and more flexible BH_4^- ion.[7] The flexibility is well illustrated in the ammonium metal borohydrides: e.g., one BH_4^- group acts as a counterion (κ^0) in the structures of $(NH_4)_3M(BH_4)_5$ (M = Mg, Mn), while four BH_4^- groups coordinate to the metal through the edge of the tetrahedron (κ^2). In the majority of the structures investigated here, the BH_4^- coordinates to the metal via the edge (κ^2) or the face (κ^3) of the tetrahedron (Table S3), which

https://dx.doi.org/10.1021/acs.inorgchem.0c01797
Inorg. Chem. XXXX, XXX, XXX−XXX

Table 3. Overview of Hydrogen Contents, Coordination Geometries, and Building Units of the Investigated Compounds

Compound	$\rho_m(H_2)$ (wt % H)	$\rho_V(H_2)$ (g H_2/L)	structure type	M^{m+} coord[a]	NH_4^+ coord[a]	BH_4^- coord[a]	building units
NH_4BH_4	24.5	157.0	NaCl		Oct (6)	Oct (6)	$[NH_4^+][BH_4^-]$
$NH_4Li(BH_4)_2$	22.1	153.1	$LiRb(BH_4)_2$	*Tet (4)*, Spl (4)	Cub (8), Bts (8), Cub (8), Bts (8)	Oct (6), Pbp (7)	$[Li(BH_4)_2]^-$ chains
$NH_4Li_2(BH_4)_3$	21.1	140.5	$Li_2M(BH_4)_3$ (M = Rb, Cs)	Tet (4)	Cta (10)	Sqa (8), Spy (5)	$[Li_2(BH_4)_3]^-$ framework
$(NH_4)_2Mg(BH_4)_4$	20.2	150.8	$K_2M(BH_4)_4$ (M = Mg, Mn)	Tet (4)	Ctp (7)	Tet (4), Pyv (4), Spy (5), Tpv (5)	isolated $[Mg(BH_4)_4]^{2-}$
$(NH_4)_3Mg(BH_4)_5$	21.1	158.2	$K_3M(BH_4)_5$ (M = Mg, Mn)	Tet (4)	Bts (8) Bsa (10)	Oct (6)	isolated $[Mg(BH_4)_4]^{2-}$
$NH_4Ca(BH_4)_3$	15.7	113.0	$RbCa(BH_4)_3$	Oct (6)	Cuo (12)	Oct (6)	$[Ca(BH_4)_6]^{4-}$ framework
$NH_4Sr(BH_4)_3$	10.7	104.3	$RbCa(BH_4)_3$	Oct (6)	Cuo (12)	Oct (6)	$[Sr(BH_4)_6]^{4-}$ framework
$NH_4Y(BH_4)_4$	12.1	128.9	$RbY(BH_4)_4$	Tet (4)	Pbp (7)	Trv (2), Tri (3), Tev (3)	Isolated $[Y(BH_4)_4]^-$
$(NH_4)_2Mn(BH_4)_4$	16.1	147.9	$K_2M(BH_4)_4$ (M = Mg, Mn)	Tet (4)	Ctp (7)	Tet (4). Pyv (4), Spy (5), Tpv (5)	isolated $[Mn(BH_4)_4]^{2-}$
$(NH_4)_3Mn(BH_4)_5$	17.6	154.4	$K_3M(BH_4)_5$ (M = Mg, Mn)	Tet (4)	Bts (8), Bsa (10)	Oct (6)	isolated $[Mn(BH_4)_4]^{2-}$
$(NH_4)_3La_2(BH_4)_9$	10.4	142.1	new structure	Oct (6)	Cuo (12)	Spy (5), Oct (6)	$[La(BH_4)_6]^{3-}$ layers
$(NH_4)_3La(BH_4)_6$	12.9	150.0	$K_3M(BH_4)_6$ (M = La, Gd)	Oct (6)	Oct (6), Con (6), Bts (8)	Tet (4), Tpv (5), Spy (5)	isolated $[La(BH_4)_6]^{3-}$
$(NH_4)_2Gd(BH_4)_5$	10.5	146.3	$K_2Gd(BH_4)_5$	Tbp (5), Spy (5)	Oct (6), Sqa (8), Boc (8)	Tri (3), Tet (4), Bva (4), Tpv (5), Oct (6)	isolated $[Gd(BH_4)_5]^{2-}$
$(NH_4)_3Gd(BH_4)_6$	12.1	152.0	$K_3M(BH_4)_6$ (M = La, Gd)	Oct (6)	Oct (6), Con (6), Bts (8)	Tet (4), Tpv (5), Spy (5)	isolated $[Gd(BH_4)_6]^{3-}$
$NH_4Mg(BH_4)_3 \cdot 2NH_3$	18.3	143.5	$LiMg(BH_4)_3 \cdot 2NH_3$	Tbp (5)	Oct (6)	Tev (3)	isolated $[Mg(NH_3)_2(BH_4)_3]^-$
$NH_4Mn(BH_4)_3 \cdot 2NH_3$	14.6	143.2	$LiMg(BH_4)_3 \cdot 2NH_3$	Tbp (5)	Oct (6)	Tev (3)	isolated $[Mn(NH_3)_2(BH_4)_3]^-$
$NH_4Y(BH_4)_4 \cdot NH_3$	12.6	138.8	new structure	Tbp (5)	Boc (8)	Tev (3)	isolated $[Y(BH_4)_4(NH_3)]^-$
$(NH_4)_2Y(BH_4)_5 \cdot NH_3$	17.0	144.3	$(NH_4)_2VF_5 \cdot H_2O$	Oct (6)	Tpv (5)	Tev (3)	isolated $[Y(BH_4)_5(NH_3)]^{2-}$
$NH_4La(BH_4)_4 \cdot NH_3$	9.9	137.9	new structure	Oct (6)	Oct (6), Csa (9)	Tev (3), Tri (3), Spl (4)	$[La(NH_3)(BH_4)_5]^{2-}$ chains
$(NH_4)_2La(BH_4)_5 \cdot NH_3BH_3$	12.2	149.0	new structure	6-fold	6-fold (6), Cap Oct (7)	Tet (4), Bvp (4), Oct (6)	isolated $[La(NH_3BH_3)(BH_4)_5]^{2-}$
$NH_4Gd(BH_4)_4 \cdot NH_3$	9.2	148.2	new structure	Oct (6)	Oct (6), Csa (9)	Tev (3), Tri (3), Spl (4)	$[Gd(NH_3)(BH_4)_5]^{2-}$ chains

[a]Coordination geometry of the ions in the structures. Hydrogen atoms are not considered. The number refers to the number of coordinating ligands: Lin (2, linear), Trv (2, trigonal planar with a vacancy), Tri (3, trigonal planar), Tev (3, tetrahedron with a vacancy), Tet (4, tetrahedron), Spl (4, square planar), Pyv (4, square pyramid with a vacancy), Bva (4, trigonal bipyramidal with an axial vacancy), Bvp (4, trigonal bipyramidal with an equatorial vacancy), Spy (5, square pyramid), Tbp (5, trigonal bipyramid), Tpv (5, trigonal prism with a vacancy), Oct (6, octahedron), Con (6, octahedron, face monocapped with a vacancy), Ctp (7, trigonal prism, square face monocapped), Pbp (7, pentagonal bipyramid), Cub (8, cube), Bts (8, trigonal prism, square face bicapped), Sqa (8, square antiprism), Boc (8, octahedron, trans-bicapped), Csa (9, square antiprism), Bsa (10, bicapped square antiprism), Cta (10, 4-capped trigonal antiprism), Cuo (12, cuboctahedron).

is the most common coordination of BH_4^- in metal borohydrides.[1,2] BH_4^- also has the ability to coordinate through the corner of the tetrahedron (κ^1), which is rare.[1] In the structure of $(NH_4)_2La(BH_4)_5 \cdot NH_3BH_3$, NH_3BH_3 coordinates to La^{3+} through one H (κ^1).

Coordination Numbers, Bond Distances, and Structural Dimensionality. The coordination number and number of coordinating ligands are shown in Figure 6a, while the M−B distance is provided in Figure 6b. More information can be found in Tables S3 and S4 in the Supporting Information. The smaller cations Li^+, Mg^{2+}, and Mn^{2+} coordinate to four or five ligands, with a CN value of 6, 8, or 10. Y^{3+} has an intermediate ionic radius; hence it has the ability to coordinate to four, five, or six ligands and has a CN value of 10 or 12. Gd^{3+} coordinates to five or six ligands with a CN value of 12, 13, or 14. The larger cations Ca^{2+}, Sr^{2+}, and La^{3+} coordinate to six ligands with CN = 12 for Ca^{2+} and Sr^{2+}, while La^{3+} shows higher coordination numbers, CN(La^{3+}) = 14 or 15. Edge-shared BH_4^- (κ^2) shows larger M−B distances in comparison to face-shared BH_4^- (κ^3), while a higher ionic radius of the metal cation results in larger M−B distances. To maintain a suitable coordination number for the metal cations, the structural dimensionality is increased if the number of BH_4^- groups is low. $NH_4Li_2(BH_4)_3$ and $NH_4M(BH_4)_3$ (M = Ca, Sr) has a low BH_4:M ratio; thus, they crystallize in 3D structures, while the BH_4:M ratio increases for $NH_4Li(BH_4)_2$ and $(NH_4)_3La_2(BH_4)_9$ and further for the 0D structures, to maintain a coordination to four, five, or six ligands, depending on the size of the metal cation.

Crystal Structure Analogues. Several of the crystal structures resemble those of K analogues, due to the similar radii of K^+ and NH_4^+, and are observed for $(NH_4)_2M(BH_4)_4$ (M^{2+} = Mg, Mn), $(NH_4)_3M(BH_4)_5$ (M^{2+} = Mg, Mn), $(NH_4)_2Gd(BH_4)_5$, and $(NH_4)_3M(BH_4)_6$ (M^{3+} = La, Gd).[21,44,48,50] Structural analogues with the slightly larger Rb^+ are observed for $NH_4Li(BH_4)_2$, $NH_4Li_2(BH_4)_3$, NH_4Ca-

https://dx.doi.org/10.1021/acs.inorgchem.0c01797
Inorg. Chem. XXXX, XXX, XXX−XXX

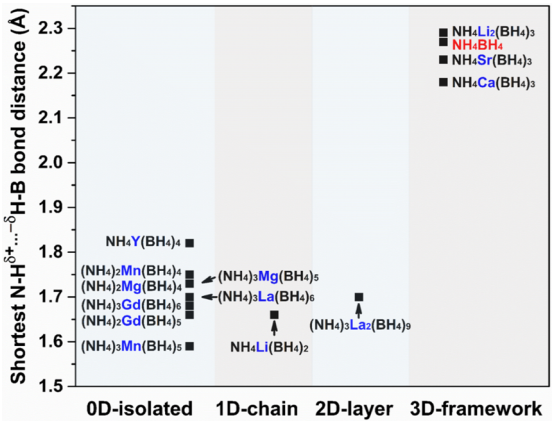

Figure 3. Shortest dihydrogen bond distance (N−H$^{\delta+}$···$^{\delta-}$H−B) and structural framework dimensionality of ammonium metal borohydrides. The H positions are obtained from DFT-optimized crystal structures.

$(BH_4)_3$, and $NH_4Y(BH_4)_4$.[31,49,93] Surprisingly, the crystal structures of $NH_4M(BH_4)_3{\cdot}2NH_3$ (M^{2+} = Mg, Mn) are isostructural with the Li^+ analogues ($r(Li^+)$ = 0.59 Å^3),[91] despite the large difference in ionic radii.[94] Interestingly, $NH_4Sr(BH_4)_3$ is isostructural with $NH_4Ca(BH_4)_3$ but different from $AB(BH_4)_3$ (A = K, Rb, Cs; B = Sr, Sm).[41,42] New structure types are observed for $(NH_4)_3La_2(BH_4)_9$, $NH_4M(BH_4)_4{\cdot}NH_3$ (M = Y, La, Gd), and $(NH_4)_2La(BH_4)_5{\cdot}NH_3BH_3$, with no resemblance to any reported metal borohydride structure.

Thermal Stability and Decomposition Mechanism. Ammonium borohydride, NH_4BH_4, slowly decomposes with a half-life of a few months (at $T \approx -34$ °C; see Figure S33), in contrast to all of the ammonium metal borohydrides, which show no loss of crystallinity after 1 year at $T \approx -34$ °C. Upon heating (~5 °C/min), an abrupt, highly exothermic decomposition of NH_4BH_4 is observed at $T \approx 68$ °C (see Figure S34). In comparison, most of the ammonium metal borohydrides, $(NH_4)_xM(BH_4)_{m+x}$, are significantly more thermally stable, while some are destabilized, which is evaluated in this section.

In situ synchrotron powder X-ray diffraction data were measured for all ammonium metal borohydrides in order to analyze the thermal decomposition mechanism, and all of the data are provided in the Supporting Information. The *in situ* SR PXD data of $NH_4Li(BH_4)_2$ measured in the temperature range −20 to +60 °C are presented in Figure 7a. At T = −20 °C, Bragg reflections are observed from $NH_4Li(BH_4)_2$ along with small reflections from excess NH_4BH_4. Upon heating, all Bragg reflections disappear simultaneously at T = 49−51 °C, suggesting the formation of amorphous compounds during decomposition. TGA-DSC-MS data revealed a mass loss of 3.8 wt %, corresponding to pure hydrogen being released in an exothermic reaction (Figure 7b). Upon further heating, an additional mass loss is observed, releasing a mixture of hydrogen and borazine.

In situ synchrotron powder X-ray diffraction, thermogravimetric analysis, differential scanning calorimetry combined with mass spectrometry (TGA-DSC-MS), and temperature-programmed photographic analysis (TPPA) data are provided for all of the remaining compounds in Figures S35−S65 in the Supporting Information along with a detailed data analysis. The decomposition temperature is defined here as the maximum peak of the DSC signal observed during heating of the sample. The thermal stability of the ammonium metal borohydrides is complex and is influenced by several factors, which will be discussed in the following.

Decomposition Temperature versus Dihydrogen Bond Lengths. The presence of dihydrogen bonds, N−H$^{\delta+}$···$^{\delta-}$H−B, facilitates the release of hydrogen at low temperatures, clearly observed by the much lower decomposition temperature of NH_4BH_4, in comparison to those of the alkali-metal borohydrides (e.g., $T_{dec}(KBH_4) \approx 600$ °C).[68,95] The decomposition of the ammonium metal borohydrides is exothermic due to the combination of $H^{\delta+}$ and $H^{\delta-}$, in contrast to the endothermic decomposition of metal borohydrides, where only hydridic $H^{\delta-}$ is present. The dihydrogen distances extracted from the DFT-optimized crystal structures (Table S5) and their relation to the thermal stability are shown in Figure 8a. The most stable compounds, e.g. $NH_4Ca(BH_4)_3$ and $NH_4Sr(BH_4)_3$, have relatively long and weak dihydrogen bonds, ~2.2 Å, whereas those with lower

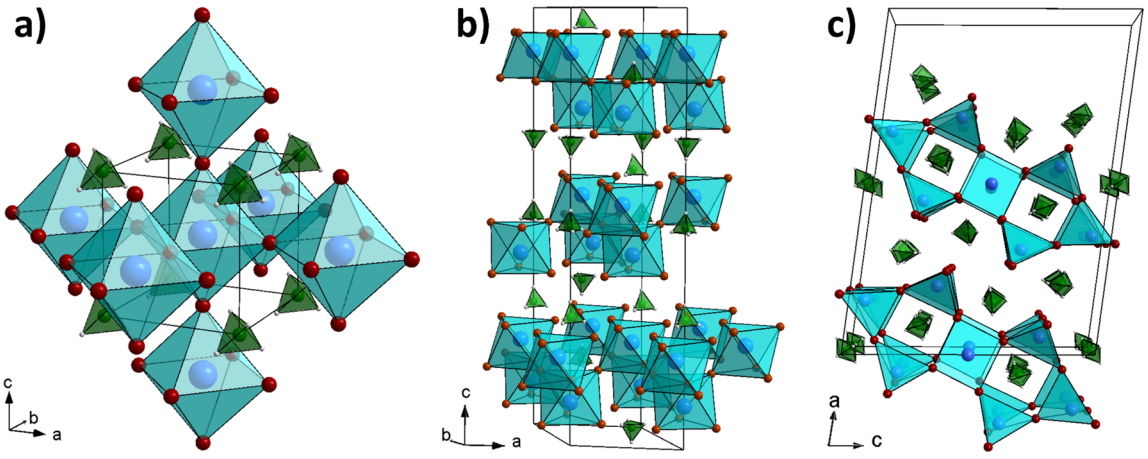

Figure 4. Crystal structures of (a) $NH_4M(BH_4)_3$ (M = Ca, Sr; three-dimensional), (b) $(NH_4)_3La_2(BH_4)_9$ (two-dimensional), (c) $NH_4Li(BH_4)_2$ (one-dimensional). Color code: M (blue), B (brown), N (green), H (gray), metal coordination sphere (light blue). H atoms in BH_4^- are omitted for clarity.

https://dx.doi.org/10.1021/acs.inorgchem.0c01797
Inorg. Chem. XXXX, XXX, XXX−XXX

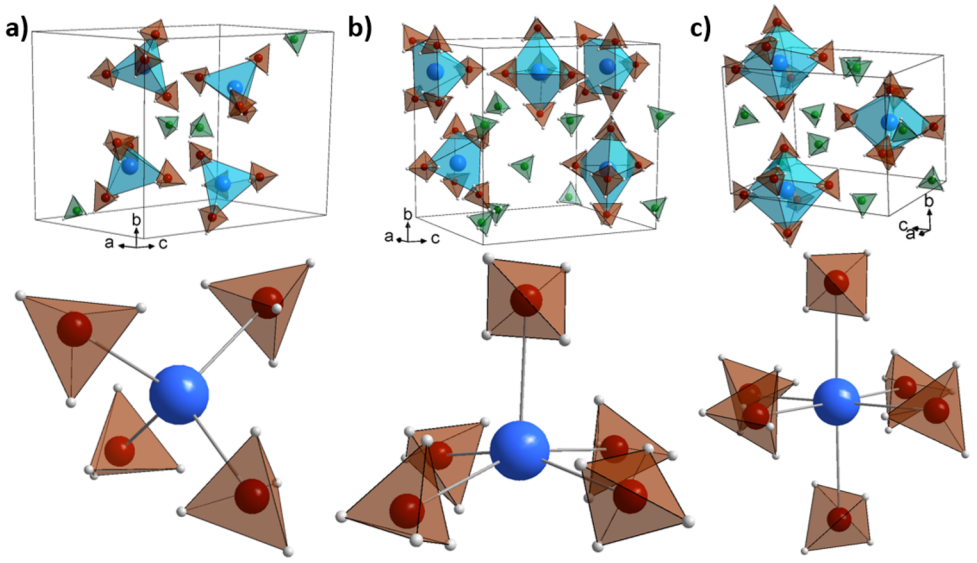

Figure 5. Crystal structures and coordination geometries of the metal cation. (a) Isolated tetrahedral complexes in $NH_4Y(BH_4)_4$. (b) Isolated square-pyramidal and trigonal-bipyramidal complexes in $(NH_4)_2Gd(BH_4)_5$. (c) Isolated octahedral complexes in $(NH_4)_3Gd(BH_4)_6$. Color code: M (blue), B (brown), N (green), H (gray), BH_4^- (brown tetrahedra).

thermal stability have significantly shorter dihydrogen bonds, ~1.59−1.82 Å.

Decomposition Temperature versus Structural Framework Dimensionality. The thermal stability of the ammonium metal borohydrides appears to be influenced by the dimensionality of the structural frameworks built from connected BH_4^- groups (Figure 8b). The 3D-framework structures are the most stable compounds (with the weakest and longest dihydrogen interactions), and the stability generally decreases with decreasing dimensionality: i.e., the stability approximately follows the order 3D framework > 2D layers > 1D chains > isolated anionic complexes. A lower structural dimensionality results in more dihydrogen, $H^{\delta+\cdots\delta-}H$, interactions. Moreover, a freer and more flexible (more dynamic) movement of BH_4^- can make it more reactive toward the NH_4^+ cation, resulting in hydrogen release through the combination of $H^{\delta+}$ and $H^{\delta-}$.

Decomposition Temperature versus Pauling Electronegativity. The thermal stability of the ammonium metal borohydrides appears to correlate inversely with the Pauling electronegativity of the metal (χ_p), as observed for the metal borohydrides: i.e., a higher χ_p value results in a lower decomposition temperature (Figure 8c).[96−98] An increased Pauling electronegativity of the metal destabilizes the borohydride group, making it more reactive toward the NH_4^+, hence resulting in lower decomposition temperatures of the ammonium metal borohydrides. Thus, ammonium metal borohydrides formed with stable metal borohydrides (with relatively high decomposition temperatures) are generally more stable (Figure 8d).

Decomposition Temperature versus Boron−Hydrogen Bond Length. The B−H bond length has been extracted from the DFT-optimized crystal structures. There is a variation in the average B−H bond length from 1.211 Å in $NH_4Ca(BH_4)_3$ to 1.225 Å in $(NH_4)_3Mn(BH_4)_5$. Elongated bonds are observed for the compounds where the metal has higher electronegativity: i.e., the metal "pulls" H away from B. Additionally, for structures with lower dimensionality, more of the B−H bonds from terminal BH_4^- are involved in the metal coordination. Hence, the B−H bond length reflects both the electronegativity of the metal and the dimensionality of the structures and correlates well with the thermal stability of the ammonium metal borohydrides; longer B−H bonds are observed for the less stable ammonium metal borohydrides (Figure 8e).

Decomposition Temperature versus Ratio between Ammonium and Borohydride, NH_4^+:BH_4^-. The thermal stability of the ammonium metal borohydrides appears to correlate with the ratio between NH_4^+ and BH_4^- in the composition of the structures (Figure 8f). The compounds with the ratio NH_4^+:BH_4^- = 1:3 are the most stable, while compounds with higher ratios, i.e. higher NH_4BH_4 content, tend to be less stable.

Decomposition Temperature versus Coordination Number of Ammonium. The most stable compounds, $NH_4Ca(BH_4)_3$, $NH_4Sr(BH_4)_3$, and $(NH_4)_3La_2(BH_4)_9$, are also the only compounds with NH_4^+ placed in a cuboctahedral coordination geometry formed by 12 nearest BH_4^- neighbors, which may enhance the thermal stability. For the remaining compounds with $CN(NH_4^+) < 12$ (Table 3) there was no correlation with the thermal stability (Figure 9a): i.e., the stabilization from the coordination environment of the NH_4^+ cation becomes weaker and other effects dominate.

Decomposition Temperature versus Structural Compression. The thermal stability versus the compression of the structures was evaluated, but no obvious correlation between these factors was observed (Figure 9b).

The thermal stability of the ammonium metal borohydrides appears to be influenced by several factors in a complex manner, as illustrated in Figures 8 and 9. In several cases only some of the ammonium metal borohydrides clearly follow a trend with a selected structural property, and others do not. This indicate that the individual structural properties have different effects on the thermal stability for the ammonium metal borohydrides: i.e., the structural property is a dominating factor in some cases. In some cases a combined effect from several structural properties may dominate the thermal stability. Other factors such as the composition, chemical

https://dx.doi.org/10.1021/acs.inorgchem.0c01797
Inorg. Chem. XXXX, XXX, XXX−XXX

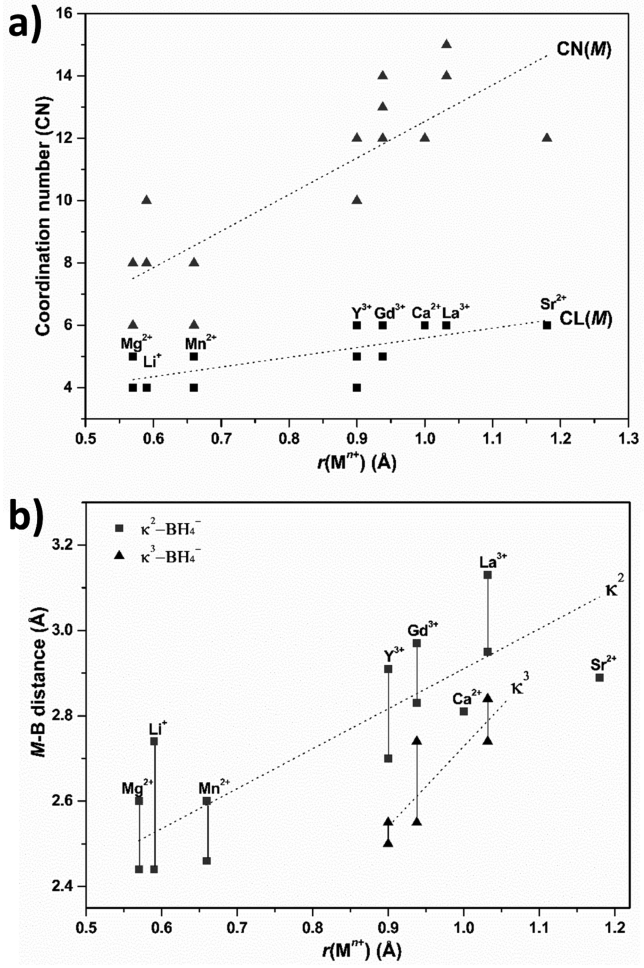

Figure 6. (a) Number of ligands coordinating to the metal (CL) and the coordination number of the metal (CN): i.e., the number of atoms coordinating to the metal. (b) Metal−boron distances and hapticities of the BH_4^-−metal coordination for the ammonium metal borohydrides as a function of the metal ionic radius. The dotted line shows the average M−B distance for the given hapticity (κ) as a function of the ionic radii.

valence, and radii of the metal cations may also influence the thermal stability. Thus, generally a combined effect from several structural properties often appears to determine the thermal stability.

Foaming. NH_4BH_4 foams heavily, and the volume expands more than 10-fold during thermolysis (Figure S35). Similarly, several of the ammonium metal borohydrides foam during decomposition, e.g. $(NH_4)_xMg(BH_4)_{2+x}$ (x = 2, 3) expands up to 50-fold (Figure S43), which often results in amorphous compounds as observed by *in situ* SR PXD. These decomposition products are often in the molten state until $T \approx 150$ °C, but the decomposition products may consist of mixtures of crystalline and molten states: e.g., as observed for the decomposition of $NH_4Y(BH_4)_4$ (Figures S53, S54, and S57). In contrast, the more stable $NH_4M(BH_4)_3$ (M = Ca, Sr) successfully suppresses foaming during decomposition; thus, crystalline compounds are observed in the subsequent decomposition steps (see Figures S44, S46, S47, and S49).

Decomposition Mechanism. The decomposition of ammonium metal borohydrides is different from that of pristine NH_4BH_4, which decomposes into $[(NH_3)_2BH_2]BH_4$, an ionic isomer of NH_3BH_3.[68]

The ammonium metal borohydrides with a ratio of NH_4:M $\leq$ 1 release pure H_2 exothermically in the first decomposition step, forming NH_3BH_3. The formed NH_3BH_3 immediately reacts with $M(BH_4)_m$, forming ammonia borane metal borohydrides; e.g., $NH_4Ca(BH_4)_3$ decomposes to form $Ca(BH_4)_2{\cdot}NH_3BH_3$ and H_2 (see eq 2).

$$NH_4Ca(BH_4)_3(s) \rightarrow Ca(BH_4)_2{\cdot}NH_3BH_3(s) + H_2(g) \quad (2)$$

Ammonium metal borohydrides with a NH_4:M ratio higher than 1 often release both diborane and hydrogen in the first decomposition step, suggesting that ammonia compounds are being formed (see Figures S40 and S42b). $(NH_4)_3Mg(BH_4)_5$ decomposes by releasing H_2 and B_2H_6 in an exothermic reaction, forming the new compound $NH_4Mg(BH_4)_3{\cdot}2NH_3$, which then further decomposes to $Mg(BH_4)_2{\cdot}2NH_3{\cdot}NH_3BH_3$ via a release of H_2 (see eq 3).

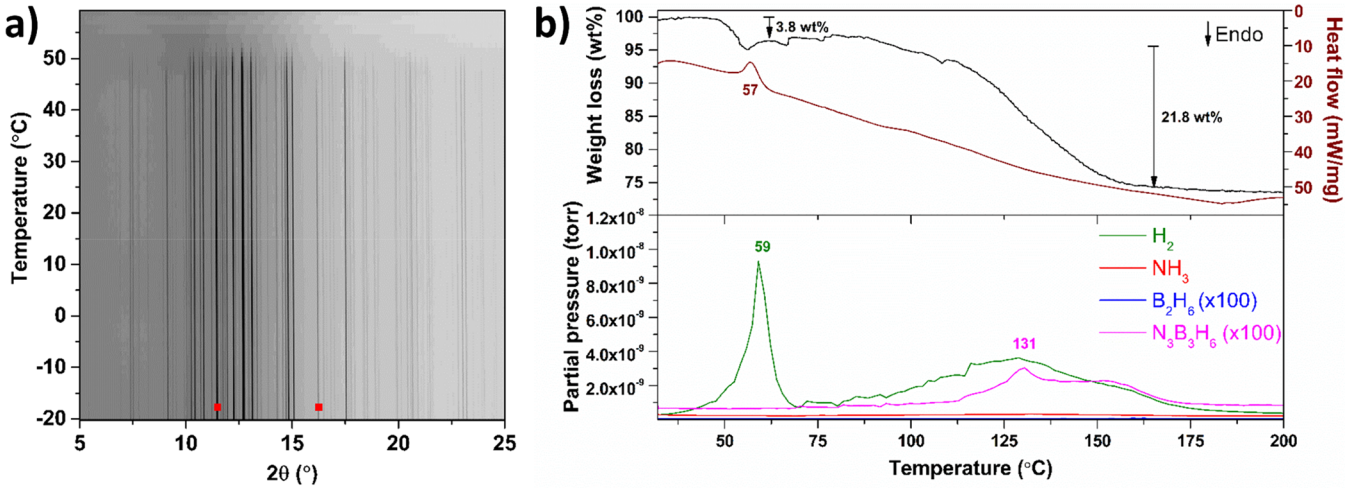

Figure 7. (a) *In situ* SR PXD of **Li11** at ESRF, heated from −20 to +60 °C ($\Delta T/\Delta t$ = 2 °C/min, p(Ar) = 1 bar, λ = 0.69449 Å). Symbols: NH_4BH_4 (red squares). The remaining diffraction peaks are assigned to $NH_4Li(BH_4)_2$. (b) TGA-DSC-MS data of **Li11** during heating from 32 to 200 °C ($\Delta T/\Delta t$ = 5 °C/min): (top)TGA data (black) and DSC data (brown); (bottom) MS signals of H_2 (green), NH_3 (red), B_2H_6 (blue), and $N_3B_3H_6$ (pink). The signals of B_2H_6 and $N_3B_3H_6$ have been amplified ×100.

https://dx.doi.org/10.1021/acs.inorgchem.0c01797
Inorg. Chem. XXXX, XXX, XXX−XXX

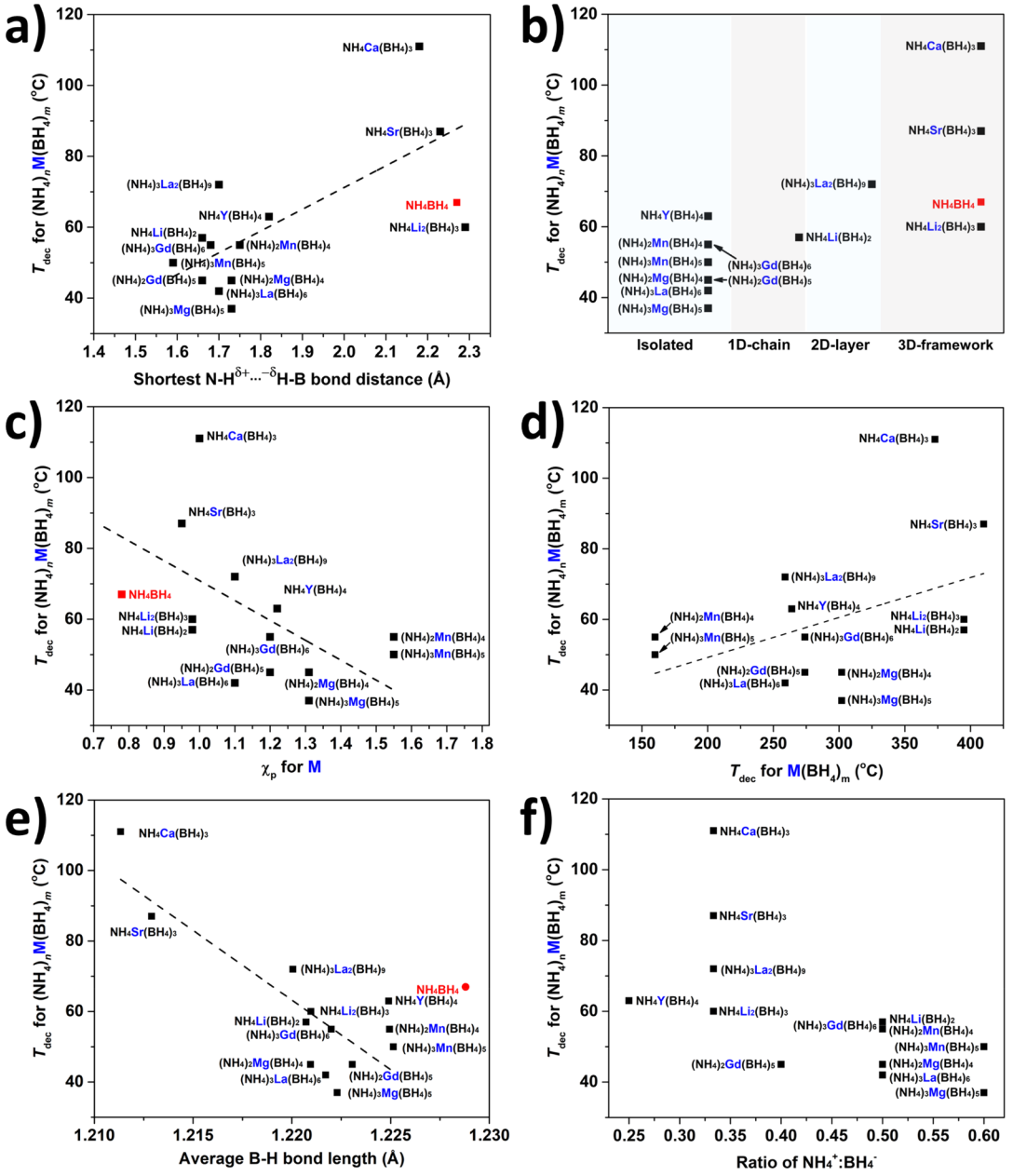

Figure 8. Decomposition temperature (T_{dec}) of the ammonium metal borohydrides, $(NH_4)_xM_y(BH_4)_{x+my}$, correlated to (a) the shortest dihydrogen bond distance, (b) the structural dimensionality, (c) the Pauling electronegativity of the metal, (d) the thermal stability of the metal borohydride, (e) the average B−H bond length in BH_4^-, and (f) the ratio between NH_4^+ and BH_4^- in the structures.

$$(NH_4)_3Mg(BH_4)_5(s) \rightarrow NH_4Mg(BH_4)_3{\cdot}2NH_3(s) + B_2H_6(g) + 2H_2(g) \rightarrow Mg(BH_4)_2{\cdot}2NH_3{\cdot}NH_3BH_3(s) + B_2H_6(g) + 3H_2(g) \quad (3)$$

Similarly, $NH_4Mn(BH_4)_3{\cdot}2NH_3$ is formed as a decomposition product from $(NH_4)_3Mn(BH_4)_5$, while $(NH_4)_2Gd(BH_4)_5$ decomposes into $NH_4Gd(BH_4)_4{\cdot}NH_3$. In contrast, $(NH_4)_3La(BH_4)_6$ decomposes into both $(NH_4)_2La(BH_4)_5{\cdot}NH_3BH_3$ and $NH_4La(BH_4)_4{\cdot}NH_3$ via a release of only H_2 or both H_2 and B_2H_6, respectively.

Suggested decomposition pathways for all the ammonium metal borohydrides investigated in this study are provided in reaction schemes E1−E21 in the Supporting Information. The decomposition contrasts with those of the bimetallic borohydrides, which dissociate during decomposition into the respective monometallic borohydrides and eventually decompose in the same manner as for the pristine compounds.[2,41,42,51,52]

Hydrogen is always released in an exothermic reaction in the first decomposition step. In general, NH_3BH_3-containing compounds are formed during the thermal decomposition of ammonium metal borohydrides when only H_2 is released, while NH_3-containing compounds are formed when B_2H_6 is also released. The decomposition products are often amorphous, and therefore the decomposition pathways have not been elucidated. The decomposition pathway of $NH_4Al(BH_4)_4$ has been studied previously, where a release of H_2, NH_3, and B_2H_6 during the decomposition was reported.[73] The main decomposition product was identified as $Al(BH_4)_3{\cdot}NHBH$, similar to the decomposition of $Al(BH_4)_3{\cdot}NH_3BH_3$,

https://dx.doi.org/10.1021/acs.inorgchem.0c01797
Inorg. Chem. XXXX, XXX, XXX−XXX

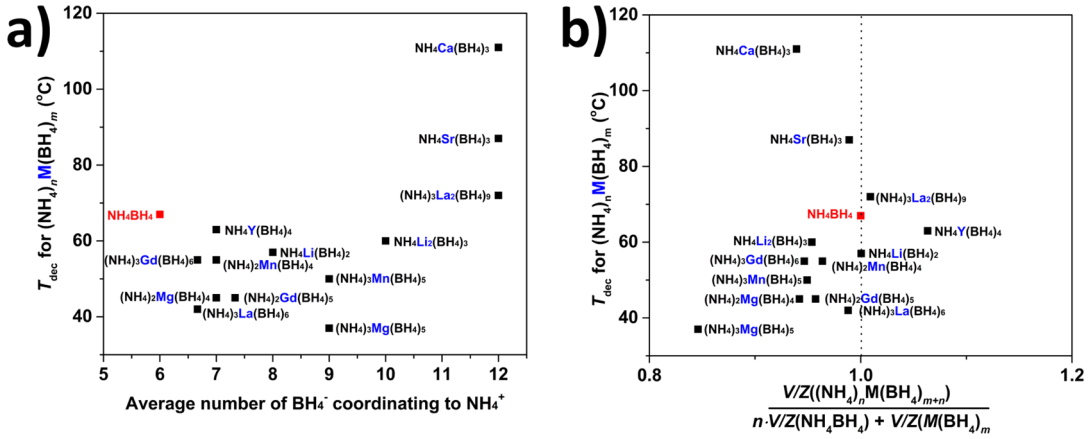

Figure 9. Decomposition temperature (T_{dec}) of the ammonium metal borohydrides, $(NH_4)_xM_y(BH_4)_{x+my}$, correlated to (a) the coordination number of NH_4 and (b) the relative structural compression.

and suggests that mainly H_2 is released during the decomposition of $NH_4Al(BH_4)_4$. $Al(BH_4)_3{\cdot}NH_3BH_3$ was not observed as a crystalline intermediate, as the sample melted during decomposition, which is also observed in several cases for the ammonium metal borohydrides presented here, such as the compounds based on M = Li, Mg, Mn, Y, La, Gd (see the section Thermal properties of ammonium metal borohydrides in the Supporting Information). In the case of $(NH_4)_3Mg(BH_4)_5$, it has been reported that amorphous boron nitride is formed during thermal decomposition already at $T \approx 220$ °C; thus, it is suggested as a potential precursor for obtaining BN.[74]

The second and third decomposition steps of ammonium metal borohydrides often take place in the temperature range T = 100−150 °C via an exothermic release of H_2, which is typically accompanied by a release of toxic gases: e.g., $N_3B_3H_6$, B_2H_6, and NH_3. This is similar to the decomposition of ammonia borane and metal borohydride ammonia borane complexes.[2,9,15,99] In cases where B_2H_6 is released in the initial decomposition step, e.g. $(NH_4)_xMg(BH_4)_{2+x}$ (x = 2, 3), hydrogen is released in the subsequent decompositions. This is similar to the case for the ammine metal borohydrides: e.g., $Mg(BH_4)_2{\cdot}xNH_3$ (x = 1, 2).[8]

CONCLUSION

Seventeen new ammonium borohydride based compounds and their crystal structures and thermal properties have been presented. Five of these compounds have new crystal structure types without any known analogue, e.g. $(NH_4)_3La_2(BH_4)_9$, with the first observed composition $(M^+)_3(M^{3+})_2(BH_4)_9$ and an unusually high coordination number of 15 for La. The structural, physical, and chemical insights into new metal borohydride type materials presented here inspire new research for tailoring of materials properties. In particular, dihydrogen interactions, $N{-}H^{\delta+}\cdots{}^{\delta-}H{-}B$, are important for the structure and properties of ammonium metal borohydrides. The dihydrogen bonding network in these materials is important for the structural stability and thermal properties. Short dihydrogen bonds, $H^{\delta+}\cdots{}^{\delta-}H$, between NH_4^+ and BH_4^-, in the range 1.59−1.82 Å are observed in structures with isolated complexes, one-dimensional chains, and two-dimensional layers. In contrast, the three-dimensional frameworks built from bridging BH_4^- units have longer dihydrogen interactions in the range 2.18−2.29 Å. The flexible borohydride complex ion is observed in the structures as counterions (κ^0), as edge-shared (κ^2) bridging ligands, and/or as terminal face-shared (κ^3) ligands. Meanwhile, NH_4^+ is considered a counterion in these compounds, as BH_4^- coordinates to the more electronegative metal cation.

The dihydrogen bonds also facilitate the release of H_2 at low temperatures (T < 100 °C), but the strength of the dihydrogen bond appears to have a minor direct influence on the thermal stability of the ammonium metal borohydrides. In fact, this work reveals that the difference in thermal stability is influenced by a range of parameters, including the structural framework dimensionality, the Pauling electronegativity of the metal, the ratio between NH_4^+ and BH_4^-, and the coordination environment of NH_4^+. The individual ammonium metal borohydrides appear to be influenced by each factor in a different fashion, and in some cases a combination of several factors may be dominating for the thermal stability.

In comparison to pristine NH_4BH_4, both stabilization and destabilization are observed. In all cases, hydrogen is released in the first decomposition step, typically below 100 °C, in an exothermic reaction, but a release of B_2H_6 is also observed in some instances. Many new compounds are obtained from the decomposition products of ammonium metal borohydrides, including ammonia borane and ammine metal borohydrides. Often these decomposition products are amorphous or are in a molten state at temperatures below 150 °C. Thus, the second and third decomposition steps resemble those of either ammine or ammonia borane metal borohydrides, releasing hydrogen along with toxic gases such as $N_3B_3H_6$, NH_3, and B_2H_6. The stable compounds $NH_4M(BH_4)_3$ (M = Ca, Sr) successfully suppress foaming during decomposition, while others often foam similarly to NH_4BH_4.

The compounds presented here are among the most hydrogen rich inorganic solid materials, which combine the two nonspherical ions NH_4^+ and BH_4^-, which are isoelectronic with natural gas, CH_4, in an extended network of dihydrogen bonds in the solid state. While the new compounds described here have very high gravimetric and volumetric hydrogen densities and release hydrogen at moderate temperatures, they possess the well-known problem of nitrogen- and boron-based compounds that their rehydrogenation is challenging and that the released gases often are contaminated by other reactive and/or poisonous components. Interesting properties may arise from the dihydrogen interactions, which can result in new types of advanced functional materials displaying, e.g.,

https://dx.doi.org/10.1021/acs.inorgchem.0c01797
Inorg. Chem. XXXX, XXX, XXX−XXX

favorable hydrogen storage properties, magnetism, luminescence, or high ionic conductivity.

■ ASSOCIATED CONTENT

Supporting Information

The Supporting Information is available free of charge at https://pubs.acs.org/doi/10.1021/acs.inorgchem.0c01797.

Crystallographic data and detailed descriptions of the crystal structures, infrared spectroscopy data, thermal analysis data, and results from DFT calculations (PDF)

Accession Codes

CCDC 1971868−1971876 and 1971878−1971886 contain the supplementary crystallographic data for this paper. These data can be obtained free of charge via www.ccdc.cam.ac.uk/data_request/cif, or by emailing data_request@ccdc.cam.ac.uk, or by contacting The Cambridge Crystallographic Data Centre, 12 Union Road, Cambridge CB2 1EZ, UK; fax: +44 1223 336033.

■ AUTHOR INFORMATION

Corresponding Author

Torben R. Jensen − *Interdisciplinary Nanoscience Center (iNANO) and Department of Chemistry, Aarhus University, DK-8000 Aarhus, Denmark;* orcid.org/0000-0002-4278-3221; Email: trj@chem.au.dk

Authors

Jakob B. Grinderslev − *Interdisciplinary Nanoscience Center (iNANO) and Department of Chemistry, Aarhus University, DK-8000 Aarhus, Denmark;* orcid.org/0000-0001-7645-1383

Lars H. Jepsen − *Interdisciplinary Nanoscience Center (iNANO) and Department of Chemistry, Aarhus University, DK-8000 Aarhus, Denmark*

Young-Su Lee − *Center for Energy Materials Research, Korea Institute of Science and Technology, Seoul 02792, Republic of Korea;* orcid.org/0000-0002-3160-6633

Kasper T. Møller − *Interdisciplinary Nanoscience Center (iNANO) and Department of Chemistry, Aarhus University, DK-8000 Aarhus, Denmark; Department of Imaging and Applied Physics, Fuels and Energy Technology Institute, Curtin University, Perth 6845, Western Australia, Australia;* orcid.org/0000-0002-1970-6703

Young Whan Cho − *Center for Energy Materials Research, Korea Institute of Science and Technology, Seoul 02792, Republic of Korea*

Radovan Černý − *Laboratory of Crystallography, DQMP, University of Geneva, 1211 Geneva, Switzerland;* orcid.org/0000-0002-9847-4372

Complete contact information is available at: https://pubs.acs.org/10.1021/acs.inorgchem.0c01797

Notes

The authors declare no competing financial interest.

■ ACKNOWLEDGMENTS

The work was supported by the Danish Research Council for Nature and Universe (DanScatt), the independent research fund of Denmark for technology and production through the projects SOS-MagBat (DFF-9041-00226B) and HyNanoBorN (DFF-4181-00462), the Carlsberg Foundation, CALIPSOplus (grant agreement 730872) from the EU Framework programme for research and innovation HORIZON 2020 and NordForsk via the project Functional Hydrides-FunHy (no. 81942). K.T.M. acknowledges The Independent Research Fund Denmark for International Postdoctoral grant 8028-00009B. The work at the Korea Institute of Science and Technology (KIST) was supported by the KIST Institutional Program (Project No. 2E29630). The authors thank the Diamond Light Source for access to beamline I11 and the local contacts Chiu Tang, Stephen Thompson, Annabelle Baker, and Sarah Day for assistance with data collection, the Swiss-Norwegian beamline BM01 at the European Synchrotron Radiation Facilities (ESRF) and the local contact Dmitry Chernyshov for assistance during the experiment, and the beamline I-711 at MAXlab, Lund, for the provision of beamtime.

■ REFERENCES

(1) Černý, R.; Schouwink, P. The Crystal Chemistry of Inorganic Metal Borohydrides and Their Relation to Metal Oxides. *Acta Crystallogr., Sect. B: Struct. Sci., Cryst. Eng. Mater.* **2015**, *71*, 619−640.

(2) Paskevicius, M.; Jepsen, L. H.; Schouwink, P.; Černý, R.; Ravnsbæk, D. B.; Filinchuk, Y.; Dornheim, M.; Besenbacher, F.; Jensen, T. R. Metal Borohydrides and Derivatives − Synthesis, Structure and Properties. *Chem. Soc. Rev.* **2017**, *46*, 1565−1634.

(3) Milanese, C.; Jensen, T. R.; Hauback, B. C.; Pistidda, C.; Dornheim, M.; Yang, H.; Lombardo, L.; Zuettel, A.; Filinchuk, Y.; Ngene, P.; de Jongh, P. E.; Buckley, C. E.; Dematteis, E. M.; Baricco, M. Complex Hydrides for Energy Storage. *Int. J. Hydrogen Energy* **2019**, *44*, 7860−7874.

(4) Grinderslev, J. B.; Møller, K. T.; Bremholm, M.; Jensen, T. R. Trends in Synthesis, Crystal Structure, and Thermal and Magnetic Properties of Rare-Earth Metal Borohydrides. *Inorg. Chem.* **2019**, *58*, 5503−5517.

(5) Richter, B.; Grinderslev, J. B.; Møller, K. T.; Paskevicius, M.; Jensen, T. R. From Metal Hydrides to Metal Borohydrides. *Inorg. Chem.* **2018**, *57*, 10768−10780.

(6) Grinderslev, J. B.; Ley, M. B.; Lee, Y.-S.; Jepsen, L. H.; Jørgensen, M.; Cho, Y. W.; Skibsted, J.; Jensen, T. R. Ammine Lanthanum and Cerium Borohydrides, $M(BH_4)_3{\cdot}nNH_3$; Trends in Synthesis, Structures, and Thermal Properties. *Inorg. Chem.* **2020**, *59*, 7768.

(7) Jepsen, L. H.; Ley, M. B.; Černý, R.; Lee, Y.-S.; Cho, Y. W.; Ravnsbæk, D.; Besenbacher, F.; Skibsted, J.; Jensen, T. R. Trends in Syntheses, Structures, and Properties for Three Series of Ammine Rare-Earth Metal Borohydrides, $M(BH_4)_3{\cdot}nNH_3$ (M = Y, Gd, and Dy). *Inorg. Chem.* **2015**, *54*, 7402−7414.

(8) Yang, Y.; Liu, Y.; Li, Y.; Gao, M.; Pan, H. Synthesis and Thermal Decomposition Behaviors of Magnesium Borohydride Ammoniates with Controllable Composition as Hydrogen Storage Materials. *Chem. - Asian J.* **2013**, *8*, 476−481.

(9) Jørgensen, M.; Lee, Y.-S.; Bjerring, M.; Jepsen, L. H.; Akbey, Ü.; Cho, Y. W.; Jensen, T. R. Disorder Induced Polymorphic Transitions in the High Hydrogen Density Compound $Sr(BH_4)_2(NH_3BH_3)_2$. *Dalton Trans.* **2018**, *47*, 16737−16746.

(10) Jepsen, L. H.; Ley, M. B.; Lee, Y.-S.; Cho, Y. W.; Dornheim, M.; Jensen, J. O.; Filinchuk, Y.; Jørgensen, J.-E.; Besenbacher, F.; Jensen, T. R. Boron−Nitrogen Based Hydrides and Reactive Composites for Hydrogen Storage. *Mater. Today* **2014**, *17*, 129−135.

(11) Jepsen, L. H.; Ley, M. B.; Filinchuk, Y.; Besenbacher, F.; Jensen, T. R. Tailoring the Properties of Ammine Metal Borohydrides for Solid-State Hydrogen Storage. *ChemSusChem* **2015**, *8*, 1452−1463.

(12) Christmann, J.; Mansouri, A.; Grinderslev, J. B.; Jensen, T. R.; Hagemann, H. Probing the Local Symmetry of Tb^{3+} in Borohydrides Using Luminescence Spectroscopy. *J. Lumin.* **2020**, *221*, 117065.

(13) Rude, L. H.; Groppo, E.; Arnbjerg, L. M.; Ravnsbæk, D. B.; Malmkjær, R. A.; Filinchuk, Y.; Baricco, M.; Besenbacher, F.; Jensen,

https://dx.doi.org/10.1021/acs.inorgchem.0c01797
Inorg. Chem. XXXX, XXX, XXX−XXX

T. R. Iodide Substitution in Lithium Borohydride, $LiBH_4$–LiI. *J. Alloys Compd.* **2011**, *509*, 8299–8305.
(14) Johnson, S. R.; David, W. I. F.; Royse, D. M.; Sommariva, M.; Tang, C. Y.; Fabbiani, F. P. A.; Jones, M. O.; Edwards, P. P. The Monoammoniate of Lithium Borohydride, $Li(NH_3)BH_4$: An Effective Ammonia Storage Compound. *Chem. - Asian J.* **2009**, *4*, 849–854.
(15) Wu, H.; Zhou, W.; Pinkerton, F. E.; Meyer, M. S.; Srinivas, G.; Yildirim, T.; Udovic, T. J.; Rush, J. J. A New Family of Metal Borohydride Ammonia Borane Complexes: Synthesis, Structures, and Hydrogen Storage Properties. *J. Mater. Chem.* **2010**, *20*, 6550–6556.
(16) Schouwink, P.; Morelle, F.; Sadikin, Y.; Filinchuk, Y.; Černý, R. Increasing Hydrogen Density with the Cation-Anion Pair BH_4^--NH_4^+ in Perovskite-Type $NH_4Ca(BH_4)_3$. *Energies* **2015**, *8*, 8286–8299.
(17) Matsuo, M.; Kuromoto, S.; Sato, T.; Oguchi, H.; Takamura, H.; Orimo, S. Sodium Ionic Conduction in Complex Hydrides with $[BH_4]^-$ and $[NH_2]^-$ Anions. *Appl. Phys. Lett.* **2012**, *100*, 203904.
(18) Higashi, S.; Miwa, K.; Aoki, M.; Takechi, K. A Novel Inorganic Solid State Ion Conductor for Rechargeable Mg Batteries. *Chem. Commun.* **2014**, *50*, 1320–1322.
(19) Jepsen, L. H.; Lee, Y.-S.; Černý, R.; Sarusie, R. S.; Cho, Y. W.; Besenbacher, F.; Jensen, T. R. Ammine Calcium and Strontium Borohydrides: Syntheses, Structures, and Properties. *ChemSusChem* **2015**, *8*, 3472–3482.
(20) Wegner, W.; van Leusen, J.; Majewski, J.; Grochala, W.; Kögerler, P. Borohydride as Magnetic Superexchange Pathway in Late Lanthanide Borohydrides. *Eur. J. Inorg. Chem.* **2019**, *2019*, 1776–1783.
(21) Schouwink, P.; Didelot, E.; Lee, Y.-S.; Mazet, T.; Černý, R. Structural and Magnetocaloric Properties of Novel Gadolinium Borohydrides. *J. Alloys Compd.* **2016**, *664*, 378–384.
(22) Zhang, T.; Wang, Y.; Song, T.; Miyaoka, H.; Shinzato, K.; Miyaoka, H.; Ichikawa, T.; Shi, S.; Zhang, X.; Isobe, S.; Hashimoto, N.; Kojima, Y. Ammonia, a Switch for Controlling High Ionic Conductivity in Lithium Borohydride Ammoniates. *Joule* **2018**, *2*, 1522–1533.
(23) Yan, Y.; Grinderslev, J. B.; Lee, Y.-S.; Jørgensen, M.; Cho, Y. W.; Černý, R.; Jensen, T. R. Ammonia-Assisted Fast Li-Ion Conductivity in a New Hemiammine Lithium Borohydride, $LiBH_4 \cdot 1/2NH_3$. *Chem. Commun.* **2020**, *56*, 3971–3974.
(24) Liu, H.; Ren, Z.; Zhang, X.; Hu, J.; Gao, M.; Pan, H.; Liu, Y. Incorporation of Ammonia Borane Groups in the Lithium Borohydride Structure Enables Ultrafast Lithium Ion Conductivity at Room Temperature for Solid-State Batteries. *Chem. Mater.* **2020**, *32*, 671–678.
(25) Yan, Y.; Dononelli, W.; Jørgensen, M.; Grinderslev, J. B.; Lee, Y.-S.; Cho, Y. W.; Černý, R.; Hammer, B.; Jensen, T. R. The Mechanism of Mg^{2+} Conduction in Ammine Magnesium Borohydride Promoted by a Neutral Molecule. *Phys. Chem. Chem. Phys.* **2020**, *22*, 9204–9209.
(26) Roedern, E.; Kühnel, R.-S.; Remhof, A.; Battaglia, C. Magnesium Ethylenediamine Borohydride as Solid-State Electrolyte for Magnesium Batteries. *Sci. Rep.* **2017**, *7*, 46189.
(27) Burankova, T.; Roedern, E.; Maniadaki, A. E.; Hagemann, H.; Rentsch, D.; Łodziana, Z.; Battaglia, C.; Remhof, A.; Embs, J. P. Dynamics of the Coordination Complexes in a Solid-State Mg Electrolyte. *J. Phys. Chem. Lett.* **2018**, *9*, 6450–6455.
(28) Kisu, K.; Kim, S.; Inukai, M.; Oguchi, H.; Takagi, S.; Orimo, S. Magnesium Borohydride Ammonia Borane as a Magnesium Ionic Conductor. *ACS Appl. Energy Mater.* **2020**, *3*, 3174–3179.
(29) Jepsen, L. H.; Ban, V.; Møller, K. T.; Lee, Y.-S.; Cho, Y. W.; Besenbacher, F.; Filinchuk, Y.; Skibsted, J.; Jensen, T. R. Synthesis, Crystal Structure, Thermal Decomposition, and ^{11}B MAS NMR Characterization of $Mg(BH_4)_2(NH_3BH_3)_2$. *J. Phys. Chem. C* **2014**, *118*, 12141–12153.
(30) Marks, S.; Heck, J. G.; Habicht, M. H.; Oña-Burgos, P.; Feldmann, C.; Roesky, P. W. $[Ln(BH_4)_2(THF)_2]$ (Ln = Eu, Yb)—A Highly Luminescent Material. Synthesis, Properties, Reactivity, and NMR Studies. *J. Am. Chem. Soc.* **2012**, *134*, 16983–16986.
(31) Schouwink, P.; Ley, M. B.; Tissot, A.; Hagemann, H.; Jensen, T. R.; Smrčok, L.; Černý, R. Structure and Properties of Complex Hydride Perovskite Materials. *Nat. Commun.* **2014**, *5*, 5706.
(32) Filinchuk, Y.; Richter, B.; Jensen, T. R.; Dmitriev, V.; Chernyshov, D.; Hagemann, H. Porous and Dense Magnesium Borohydride Frameworks: Synthesis, Stability, and Reversible Absorption of Guest Species. *Angew. Chem., Int. Ed.* **2011**, *50*, 11162–11166.
(33) Dovgaliuk, I.; Nouar, F.; Serre, C.; Filinchuk, Y.; Chernyshov, D. Cooperative Adsorption by Porous Frameworks: Diffraction Experiment and Phenomenological Theory. *Chem. - Eur. J.* **2017**, *23*, 17714–17720.
(34) Paskevicius, M.; Richter, B.; Polański, M.; Thompson, S. P.; Jensen, T. R. Sulfurized Metal Borohydrides. *Dalton Trans.* **2016**, *45*, 639–645.
(35) Wegner, W.; Jaroń, T.; Grochala, W. Preparation of a Series of Lanthanide Borohydrides and Their Thermal Decomposition to Refractory Lanthanide Borides. *J. Alloys Compd.* **2018**, *744*, 57–63.
(36) Chaikin, S. W.; Brown, W. G. Reduction of Aldehydes, Ketones and Acid Chlorides by Sodium Borohydride. *J. Am. Chem. Soc.* **1949**, *71*, 122–125.
(37) Kollonitsch, J.; Fuchs, O.; Gábor, V. New and Known Complex Borohydrides and Some of Their Applications in Organic Syntheses. *Nature* **1954**, *173*, 125–126.
(38) Heere, M.; Hansen, A.-L.; Payandeh, S.; Aslan, N.; Gizer, G.; Sørby, M. H.; Hauback, B. C.; Pistidda, C.; Dornheim, M.; Lohstroh, W. Dynamics of Porous and Amorphous Magnesium Borohydride to Understand Solid State Mg-Ion-Conductors. *Sci. Rep.* **2020**, *10*, 9080.
(39) Hagemann, H. Boron Hydrogen Compounds for Hydrogen Storage and as Solid Ionic Conductors. *Chimia* **2019**, *73*, 868–873.
(40) Hirscher, M.; Yartys, V. A.; Baricco, M.; Bellosta von Colbe, J.; Blanchard, D.; Bowman, R. C.; Broom, D. P.; Buckley, C. E.; Chang, F.; Chen, P.; Cho, Y. W.; Crivello, J.-C.; Cuevas, F.; David, W. I. F.; de Jongh, P. E.; Denys, R. V.; Dornheim, M.; Felderhoff, M.; Filinchuk, Y.; Froudakis, G. E.; Grant, D. M.; Gray, E. M.; Hauback, B. C.; He, T.; Humphries, T. D.; Jensen, T. R.; Kim, S.; Kojima, Y.; Latroche, M.; Li, H.-W.; Lototskyy, M. V.; Makepeace, J. W.; Møller, K. T.; Naheed, L.; Ngene, P.; Noréus, D.; Nygård, M. M.; Orimo, S.; Paskevicius, M.; Pasquini, L.; Ravnsbæk, D. B.; Veronica Sofianos, M.; Udovic, T. J.; Vegge, T.; Walker, G. S.; Webb, C. J.; Weidenthaler, C.; Zlotea, C. Materials for Hydrogen-Based Energy Storage – Past, Recent Progress and Future Outlook. *J. Alloys Compd.* **2020**, *827*, 153548.
(41) Møller, K. T.; Jørgensen, M.; Fogh, A. S.; Jensen, T. R. Perovskite Alkali Metal Samarium Borohydrides: Crystal Structures and Thermal Decomposition. *Dalton Trans.* **2017**, *46*, 11905–11912.
(42) Møller, K. T.; Ley, M. B.; Schouwink, P.; Černý, R.; Jensen, T. R. Synthesis and Thermal Stability of Perovskite Alkali Metal Strontium Borohydrides. *Dalton Trans.* **2016**, *45*, 831–840.
(43) Payandeh GharibDoust, S.; Ravnsbæk, D. B.; Cerny, R.; Jensen, T. R. Synthesis, Structure and Properties of Bimetallic Sodium Rare-Earth (RE) Borohydrides, $NaRE(BH_4)_4$, RE = Ce, Pr, Er or Gd. *Dalton Trans.* **2017**, *46*, 13421–13431.
(44) Payandeh GharibDoust, S.; Heere, M.; Sørby, M. H.; Ley, M. B.; Ravnsbæk, D. B.; Hauback, B.ør. C.; Cerny, R.; Jensen, T. R. Synthesis, Structure and Properties of New Bimetallic Sodium and Potassium Lanthanum Borohydrides. *Dalton Trans.* **2016**, *45*, 19002–19011.
(45) Heere, M.; GharibDoust, S. P.; Sørby, M. H.; Frommen, C.; Jensen, T. R.; Hauback, B.ør. C. In Situ Investigations of Bimetallic Potassium Erbium Borohydride. *Int. J. Hydrogen Energy* **2017**, *42*, 22468–22474.
(46) Dovgaliuk, I.; Ban, V.; Sadikin, Y.; Černý, R.; Aranda, L.; Casati, N.; Devillers, M.; Filinchuk, Y. The First Halide-Free Bimetallic Aluminum Borohydride: Synthesis, Structure, Stability, and Decomposition Pathway. *J. Phys. Chem. C* **2014**, *118*, 145–153.
(47) Roedern, E.; Lee, Y.-S.; Ley, M. B.; Park, K.; Whan Cho, Y.; Skibsted, J.; Jensen, R.; Solid State, T. Synthesis, Structural Characterization and Ionic Conductivity of Bimetallic Alkali-Metal

https://dx.doi.org/10.1021/acs.inorgchem.0c01797
Inorg. Chem. XXXX, XXX, XXX–XXX

Yttrium Borohydrides $MY(BH_4)_4$ (M = Li and Na). *J. Mater. Chem. A* **2016**, *4*, 8793−8802.
(48) Schouwink, P.; D'Anna, V.; Ley, M. B.; Lawson Daku, L. M.; Richter, B.; Jensen, T. R.; Hagemann, H.; Černý, R. Bimetallic Borohydrides in the System $M(BH_4)_2$−KBH_4 (M = Mg, Mn): On the Structural Diversity. *J. Phys. Chem. C* **2012**, *116*, 10829−10840.
(49) Schouwink, P.; Smrčok, L.; Černý, R. Role of the Li^+ Node in the Li-BH_4 Substructure of Double-Cation Tetrahydroborates. *Acta Crystallogr., Sect. B: Struct. Sci., Cryst. Eng. Mater.* **2014**, *70*, 871−878.
(50) Brighi, M.; Schouwink, P.; Sadikin, Y.; Černý, R. Fast Ion Conduction in Garnet-Type Metal Borohydrides $Li_3K_3Ce_2(BH_4)_{12}$ and $Li_3K_3La_2(BH_4)_{12}$. *J. Alloys Compd.* **2016**, *662*, 388−395.
(51) Ravnsbæk, D. B.; Sørensen, L. H.; Filinchuk, Y.; Besenbacher, F.; Jensen, T. R. Screening of Metal Borohydrides by Mechanochemistry and Diffraction. *Angew. Chem., Int. Ed.* **2012**, *51*, 3582−3586.
(52) Ravnsbæk, D.; Filinchuk, Y.; Cerenius, Y.; Jakobsen, H. J.; Besenbacher, F.; Skibsted, J.; Jensen, T. R. A Series of Mixed-Metal Borohydrides. *Angew. Chem., Int. Ed.* **2009**, *48*, 6659−6663.
(53) Černý, R.; Severa, G.; Ravnsbæk, D. B.; Filinchuk, Y.; D'Anna, V.; Hagemann, H.; Haase, D.; Jensen, C. M.; Jensen, T. R. $NaSc(BH_4)_4$: A Novel Scandium-Based Borohydride. *J. Phys. Chem. C* **2010**, *114*, 1357−1364.
(54) Wegner, W.; Jaroń, T.; Grochala, W. Polymorphism and Hydrogen Discharge from Holmium Borohydride, $Ho(BH_4)_3$, and $KHo(BH_4)_4$. *Int. J. Hydrogen Energy* **2014**, *39*, 20024−20030.
(55) Olsen, J. E.; Frommen, C.; Sørby, M. H.; Hauback, B. C. Crystal Structures and Properties of Solvent-Free $LiYb(BH_4)_{4-x}Cl_x$, $Yb(BH_4)_3$ and $Yb(BH_4)_{2-x}Cl_x$. *RSC Adv.* **2013**, *3*, 10764−10774.
(56) Olsen, J. E.; Frommen, C.; Jensen, T. R.; Riktor, M. D.; Sørby, M. H.; Hauback, B. C. Structure and Thermal Properties of Composites with RE-Borohydrides (RE = La, Ce, Pr, Nd, Sm, Eu, Gd, Tb, Er, Yb or Lu) and $LiBH_4$. *RSC Adv.* **2014**, *4*, 1570−1582.
(57) Frommen, C.; Sørby, M. H.; Heere, M.; Humphries, T. D.; Olsen, J. E.; Hauback, B. C. Rare Earth Borohydrides—Crystal Structures and Thermal Properties. *Energies* **2017**, *10*, 2115.
(58) Cerny, R.; Ravnsbæk, D. B.; Severa, G.; Filinchuk, Y.; D' Anna, V.; Hagemann, H.; Haase, D.; Skibsted, J.; Jensen, C. M.; Jensen, T. R. Structure and Characterization of $KSc(BH_4)_4$. *J. Phys. Chem. C* **2010**, *114*, 19540−19549.
(59) Wegner, W.; Jaroń, T.; Grochala, W. $MYb(BH_4)_4$ (M = K, Na) from Laboratory X-Ray Powder Data. *Acta Crystallogr., Sect. C: Cryst. Struct. Commun.* **2013**, *69*, 1289−1291.
(60) Černý, R.; Ravnsbæk, D. B.; Schouwink, P.; Filinchuk, Y.; Penin, N.; Teyssier, J.; Smrčok, L.; Jensen, T. R. Potassium Zinc Borohydrides Containing Triangular $[Zn(BH_4)_3]^-$ and Tetrahedral $[Zn(BH_4)_XCl_{4-x}]^{2-}$ Anions. *J. Phys. Chem. C* **2012**, *116*, 1563−1571.
(61) Jaroń, T.; Wegner, W.; Grochala, W. $M[Y(BH_4)_4]$ and $M_2Li[Y(BH_4)_{6-x}Cl_x]$ (M = Rb, Cs): New Borohydride Derivatives of Yttrium and Their Hydrogen Storage Properties. *Dalton Trans.* **2013**, *42*, 6886−6893.
(62) Jaroń, T.; Wegner, W.; Fijałkowski, K. J.; Leszczyński, P. J.; Grochala, W. Facile Formation of Thermodynamically Unstable Novel Borohydride Materials by a Wet Chemistry Route. *Chem. - Eur. J.* **2015**, *21*, 5689−5692.
(63) Jaroń, T.; Orłowski, P. A.; Wegner, W.; Fijałkowski, K. J.; Leszczyński, P. J.; Grochala, W. Hydrogen Storage Materials: Room-Temperature Wet-Chemistry Approach toward Mixed-Metal Borohydrides. *Angew. Chem., Int. Ed.* **2015**, *54*, 1236−1239.
(64) Starobrat, A.; Jaroń, T.; Grochala, W. Two New Derivatives of Scandium Borohydride, $MSc(BH_4)_4$, M = Rb, Cs, Prepared via a One-Pot Solvent-Mediated Method. *Dalton Trans.* **2019**, *48*, 11829−11837.
(65) Hagemann, H.; Longhini, M.; Kaminski, J. W.; Wesolowski, T. A.; Černý, R.; Penin, N.; Sørby, M. H.; Hauback, B. C.; Severa, G.; Jensen, C. M. $LiSc(BH_4)_4$: A Novel Salt of Li^+ and Discrete $Sc(BH_4)^{4-}$ Complex Anions. *J. Phys. Chem. A* **2008**, *112*, 7551−7555.
(66) Nickels, E. A.; Jones, M. O.; David, W. I. F.; Johnson, S. R.; Lowton, R. L.; Sommariva, M.; Edwards, P. P. Tuning the Decomposition Temperature in Complex Hydrides: Synthesis of a Mixed Alkali Metal Borohydride. *Angew. Chem.* **2008**, *120*, 2859−2861.
(67) Ley, M. B.; Roedern, E.; Jensen, T. R. Eutectic Melting of $LiBH_4$−KBH_4. *Phys. Chem. Chem. Phys.* **2014**, *16*, 24194−24199.
(68) Karkamkar, A.; Kathmann, S. M.; Schenter, G. K.; Heldebrant, D. J.; Hess, N.; Gutowski, M.; Autrey, T. Thermodynamic and Structural Investigations of Ammonium Borohydride, a Solid with a Highest Content of Thermodynamically and Kinetically Accessible Hydrogen. *Chem. Mater.* **2009**, *21*, 4356−4358.
(69) Bowden, M.; Heldebrant, D. J.; Karkamkar, A.; Proffen, T.; Schenter, G. K.; Autrey, T. The Diammoniate of Diborane: Crystal Structure and Hydrogen Release. *Chem. Commun.* **2010**, *46*, 8564−8566.
(70) Nielsen, T. K.; Karkamkar, A.; Bowden, M.; Besenbacher, F.; Jensen, T. R.; Autrey, T. Methods to Stabilize and Destabilize Ammonium Borohydride. *Dalton Trans.* **2013**, *42*, 680−687.
(71) Filippov, S.; Grinderslev, J. B.; Andersson, M. S.; Armstrong, J.; Karlsson, M.; Jensen, T. R.; Klarbring, J.; Simak, S. I.; Häussermann, U. Analysis of Dihydrogen Bonding in Ammonium Borohydride. *J. Phys. Chem. C* **2019**, *123*, 28631−28639.
(72) Starobrat, A.; Jaroń, T.; Grochala, W. New Hydrogen-Rich Ammonium Metal Borohydrides, $NH_4[M(BH_4)_4]$, M = Y, Sc, Al, as Potential H_2 Sources. *Dalton Trans.* **2018**, *47*, 4442−4448.
(73) Dovgaliuk, I.; Safin, D. A.; Tumanov, N. A.; Morelle, F.; Moulai, A.; Černý, R.; Łodziana, Z.; Devillers, M.; Filinchuk, Y. Solid Aluminum Borohydrides for Prospective Hydrogen Storage. *ChemSusChem* **2017**, *10*, 4725−4734.
(74) Wegner, W.; Fijalkowski, K. J.; Grochala, W. A Low Temperature Pyrolytic Route to Amorphous Quasi-Hexagonal Boron Nitride from Hydrogen Rich $(NH_4)_3Mg(BH_4)_5$. *Dalton Trans.* **2020**, *49*, 336−342.
(75) Parry, R. W.; Schultz, D. R.; Girardot, P. R. The Preparation and Properties of Hexamminecobalt(III) Borohydride, Hexamminechromium(III) Borohydride and Ammonium Borhydride. *J. Am. Chem. Soc.* **1958**, *80*, 1−3.
(76) Ley, M. B.; Paskevicius, M.; Schouwink, P.; Richter, B.; Sheppard, D. A.; Buckley, C. E.; Jensen, T. R. Novel Solvates $M(BH_4)_3S(CH_3)_2$ and Properties of Halide-Free $M(BH_4)_3$ (M = Y or Gd). *Dalton Trans.* **2014**, *43*, 13333−13342.
(77) Richter, B.; Ravnsbæk, D. B.; Tumanov, N.; Filinchuk, Y.; Jensen, T. R. Manganese Borohydride; Synthesis and Characterization. *Dalton Trans.* **2015**, *44*, 3988−3996.
(78) Favre-Nicolin, V.; Černý, R. FOX, "Free Objects for Crystallography": A Modular Approach to Ab Initio Structure Determination from Powder Diffraction. *J. Appl. Crystallogr.* **2002**, *35*, 734−743.
(79) Rodriguez-Carvajal, J. *FULLPROF SUITE*; LLB Sacley & LCSIM Rennes: 2003.
(80) Spek, A. L. Structure Validation in Chemical Crystallography. *Acta Crystallogr., Sect. D: Biol. Crystallogr.* **2009**, *65*, 148−155.
(81) Kresse, G.; Furthmüller, J. Efficient Iterative Schemes for Ab Initio Total-Energy Calculations Using a Plane-Wave Basis Set. *Phys. Rev. B: Condens. Matter Mater. Phys.* **1996**, *54*, 11169−11186.
(82) Lee, K.; Murray, É. D.; Kong, L.; Lundqvist, B. I.; Langreth, D. C. Higher-Accuracy van Der Waals Density Functional. *Phys. Rev. B: Condens. Matter Mater. Phys.* **2010**, *82*, No. 081101.
(83) Klimeš, J.; Bowler, D. R.; Michaelides, A. Van Der Waals Density Functionals Applied to Solids. *Phys. Rev. B: Condens. Matter Mater. Phys.* **2011**, *83*, 195131.
(84) Blöchl, P. E. Projector Augmented-Wave Method. *Phys. Rev. B: Condens. Matter Mater. Phys.* **1994**, *50*, 17953−17979.
(85) Paskevicius, M.; Ley, M. B.; Sheppard, D. A.; Jensen, T. R.; Buckley, C. E. Eutectic Melting in Metal Borohydrides. *Phys. Chem. Chem. Phys.* **2013**, *15*, 19774−19789.
(86) Huot, J.; Cuevas, F.; Deledda, S.; Edalati, K.; Filinchuk, Y.; Grosdidier, T.; Hauback, B. C.; Heere, M.; Jensen, T. R.; Latroche, M.; Sartori, S. Mechanochemistry of Metal Hydrides: Recent Advances. *Materials* **2019**, *12*, 2778.

https://dx.doi.org/10.1021/acs.inorgchem.0c01797
Inorg. Chem. XXXX, XXX, XXX−XXX

(87) D'Anna, V.; Spyratou, A.; Sharma, M.; Hagemann, H. FT-IR Spectra of Inorganic Borohydrides. *Spectrochim. Acta, Part A* **2014**, *128*, 902−906.
(88) D'Anna, V.; Lawson Daku, L. M.; Hagemann, H. Quantitative Spectra−Structure Relations for Borohydrides. *J. Phys. Chem. C* **2015**, *119*, 21868−21874.
(89) Crabtree, R. H.; Siegbahn, P. E. M.; Eisenstein, O.; Rheingold, A. L.; Koetzle, T. F. A New Intermolecular Interaction: Unconventional Hydrogen Bonds with Element−Hydride Bonds as ProtonAcceptor. *Acc. Chem. Res.* **1996**, *29*, 348−354.
(90) Schouwink, P.; Hagemann, H.; Embs, J. P.; D'Anna, V.; Černý, R. Di-Hydrogen Contact Induced Lattice Instabilities and Structural Dynamics in Complex Hydride Perovskites. *J. Phys.: Condens. Matter* **2015**, *27*, 265403.
(91) Shannon, R. D. Revised Effective Ionic Radii and Systematic Studies of Interatomic Distances in Halides and Chalcogenides. *Acta Crystallogr., Sect. A: Cryst. Phys., Diffr., Theor. Gen. Crystallogr.* **1976**, *32*, 751−767.
(92) Sidey, V. On the Effective Ionic Radii for Ammonium. *Acta Crystallogr., Sect. B: Struct. Sci., Cryst. Eng. Mater.* **2016**, *72*, 626−633.
(93) Jaroń, T.; Grochala, W. Probing Lewis Acidity of $Y(BH_4)_3$ via Its Reactions with MBH_4 (M = Li, Na, K, NMe_4). *Dalton Trans.* **2011**, *40*, 12808−12817.
(94) Sun, W.; Chen, X.; Gu, Q.; Wallwork, K. S.; Tan, Y.; Tang, Z.; Yu, X. A New Ammine Dual-Cation (Li, Mg) Borohydride: Synthesis, Structure, and Dehydrogenation Enhancement. *Chem. - Eur. J.* **2012**, *18*, 6825−6834.
(95) Whiteside, A.; Xantheas, S. S.; Gutowski, M. Is Electronegativity a Useful Descriptor for the Pseudo-Alkali Metal NH_4? *Chem. - Eur. J.* **2011**, *17*, 13197−13205.
(96) Møller, K. T.; Sheppard, D.; Ravnsbæk, D. B.; Buckley, C. E.; Akiba, E.; Li, H.-W.; Jensen, T. R. Complex Metal Hydrides for Hydrogen, Thermal and Electrochemical Energy Storage. *Energies* **2017**, *10*, 1645.
(97) Schrauzer, G. N. Über ein Periodensystem der Metallboranate. *Naturwissenschaften* **1955**, *42*, 438−438.
(98) Nakamori, Y.; Miwa, K.; Ninomiya, A.; Li, H.; Ohba, N.; Towata, S.; Züttel, A.; Orimo, S. Correlation between Thermodynamical Stabilities of Metal Borohydrides and Cation Electronegativites: First-Principles Calculations and Experiments. *Phys. Rev. B: Condens. Matter Mater. Phys.* **2006**, *74*, No. 045126.
(99) Chen, X.; Yuan, F.; Gu, Q.; Yu, X. Synthesis, Structures and Hydrogen Storage Properties of Two New H-Enriched Compounds: $Mg(BH_4)_2(NH_3BH_3)_2$ and $Mg(BH_4)_2{\cdot}(NH_3)_2(NH_3BH_3)$. *Dalton Trans.* **2013**, *42*, 14365−14368.

https://dx.doi.org/10.1021/acs.inorgchem.0c01797
Inorg. Chem. XXXX, XXX, XXX−XXX